Hybrid Approach for Understanding the Thermoelastic Response of CFRP Multidirectional Laminates

Rafael Ruiz Iglesias

R. Cappello, G. Ólafsson, O.T. Thomsen and J.M. Dulieu-Barton

PhD Student

THERMOELASTIC STRESS ANALYSIS (TSA)

T_0 ~ *Mean temperature*
ρ ~ *Density*
C_p ~ *Specific heat capacity*
α_1 *and* α_2 ~ *Thermal expansion coefficients in 1,2*
$\Delta\sigma_1$ *and* $\Delta\sigma_2$ ~ *Stress variation in 1,2*
$[Q]_{1,2}$ ~ *Stiffness matrix*
$[T]$ ~ *Transformation matrix*
$[\Delta\varepsilon_{xy}]$ ~ *Strain variation in x,y*

Stress variation (Δσ) is required to obtain the **thermoelastic response** of a material:

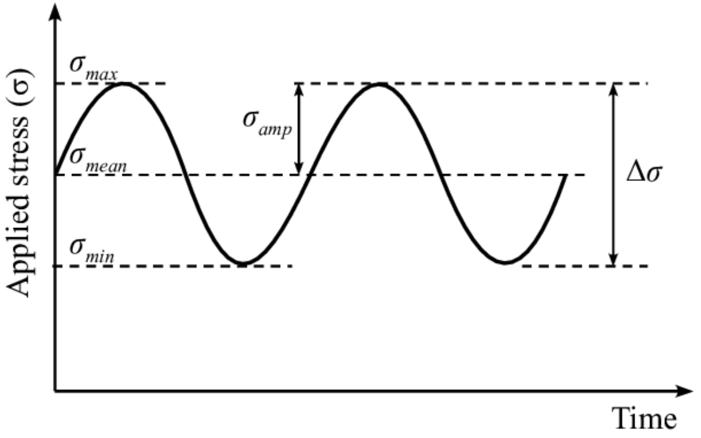

$$\Delta T = \frac{-T_0}{\rho C_p}(\alpha_1\Delta\sigma_1+\alpha_2\Delta\sigma_2) = \frac{-T_0}{\rho C_p}\left([\alpha]^T_{1,2}[Q]_{1,2}[T][\Delta\varepsilon]_{xy}\right)$$

Simplified for orthotropic composite lamina (as $\alpha_6 = 0$)

HEAT TRANSFER? → **Information from different plies?**

* We can look at each ply's stresses measuring the temperature

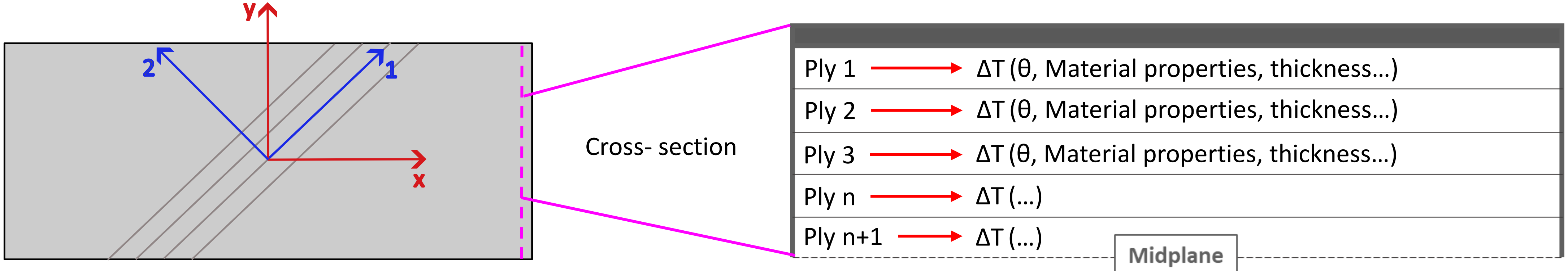

Cross-section of multi-directional symmetric laminate

1,2: Ply coordinate system

x,y: Laminate coordinate system

Why composites? Used for structural applications: Damage and features can be located in the **surface and subsurface**

MOTIVATION OF THE RESEARCH

Experimental Plan

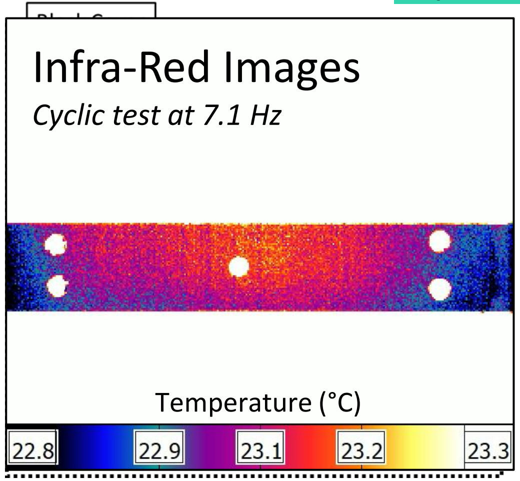

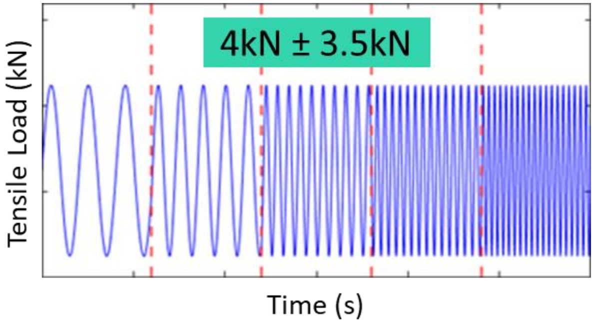

Cyclic test **below FPF**

Loading frequency (Hz): 0.5, 1.1, 2.1, 3.1, 4.1, 5.1, 7.1, 10.1… 30.1

CFRP IM7/8552: Heat transfer occurring at low frequencies [1]

Widely used in the aerospace industry

Increased complexity

25. Thermo and Infrared (Hemlock/Oak)– **Tuesday 4th (9:40 AM–10:00 AM)**
Validation of a Numerical Model for Predictions of the Thermoelastic Effect in Laminated Composite Structures #17570 R. Cappello

Through thickness and in-plane gradients

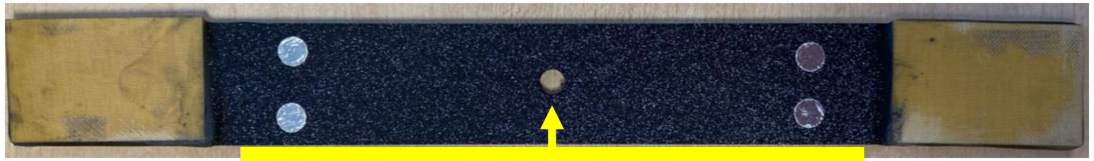

Hole induces a **3D stress state**

INTEREST → Understand the thermomechanical response of multidirectional (MD) CFRP under **3D stress states**

- Verify the thermoelastic results using thermomechanical modelling approaches → Tune loading frequency
- Quantitative analysis using both experimental and modelling data fusion to understand the condition of the material

Why is it important? **NEW & RELIABLE TOOL** for quantitative applications of TSA to laminates with complex stress states

[1] Jiménez-Fortunato I., Bull DJ., Thomsen OT., Dulieu-Barton JM. On the source of the thermoelastic response from orthotropic fibre reinforced composite laminates. Composites Part A: Applied Science and Manufacturing

MATERIAL: MULTIDIRECTIONAL CFRPs

Manufacturing was done in the autoclave following the manufacturers cycle

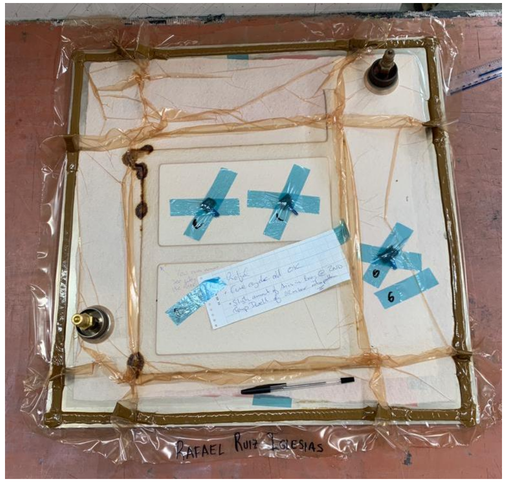

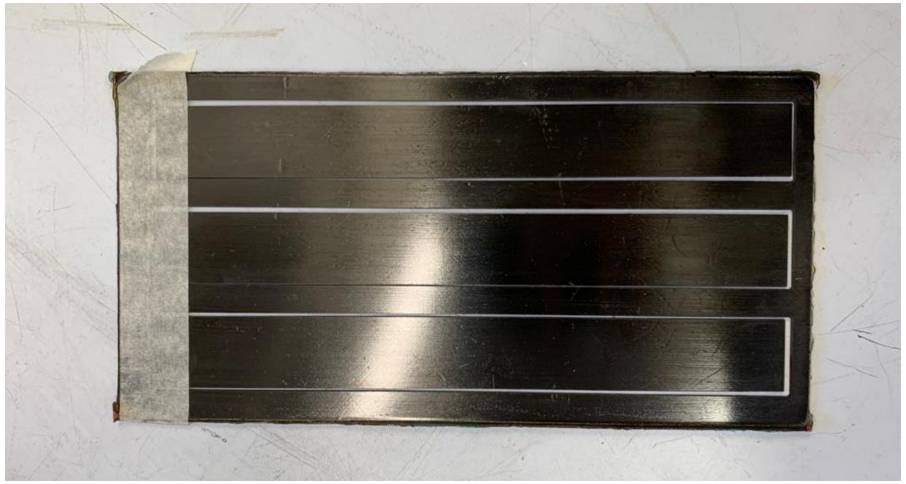

<u>Multidirectional laminates</u>

- CFRP $[0,45,-45,0,0,0]_S$
- CFRP $[0,0,0,45,-45,0]_S$

The resin plays a **<u>fundamental role in TSA</u>** and its effect must be addressed [2]

[2] Zhang D., Enke NF., Sandor BI. Thermographic stress analysis of composite materials. Experimental Mechanics.

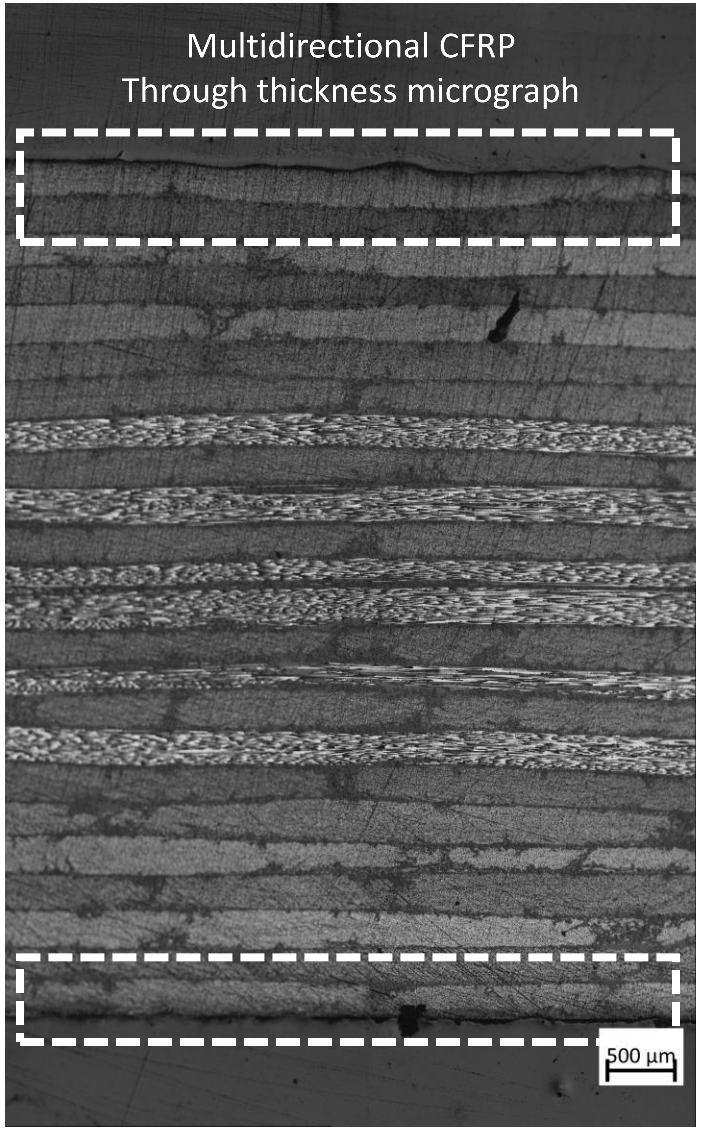

MATERIAL: MULTIDIRECTIONAL CFRPs

Manufacturing was done in the autoclave following the manufacturers cycle

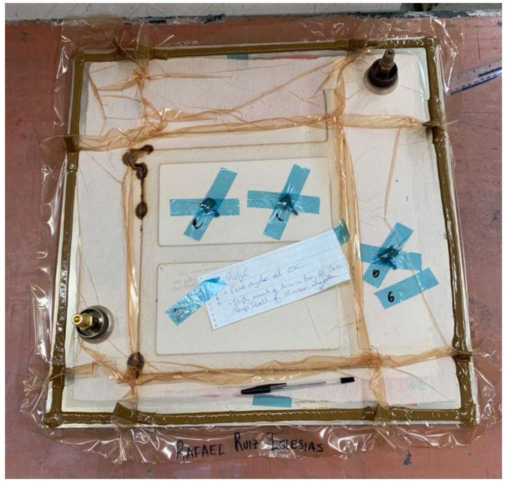

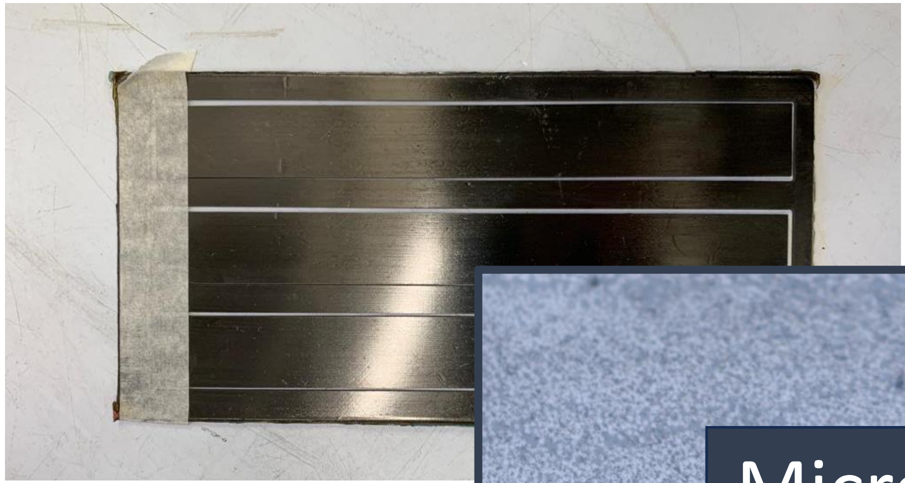

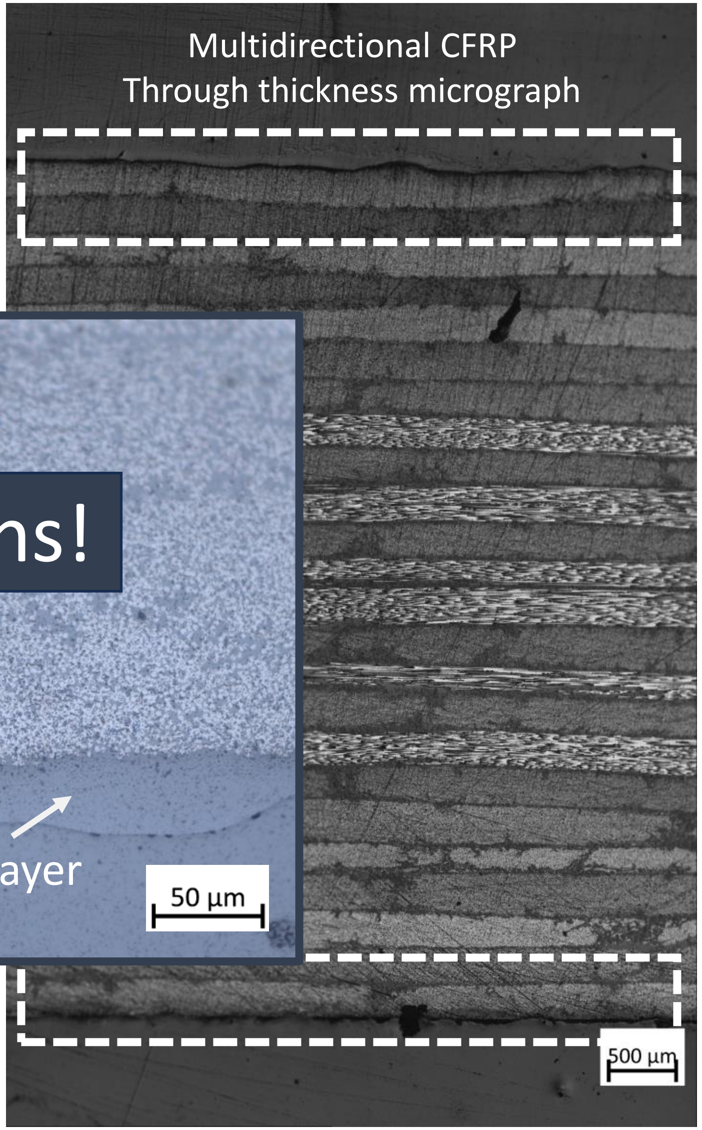

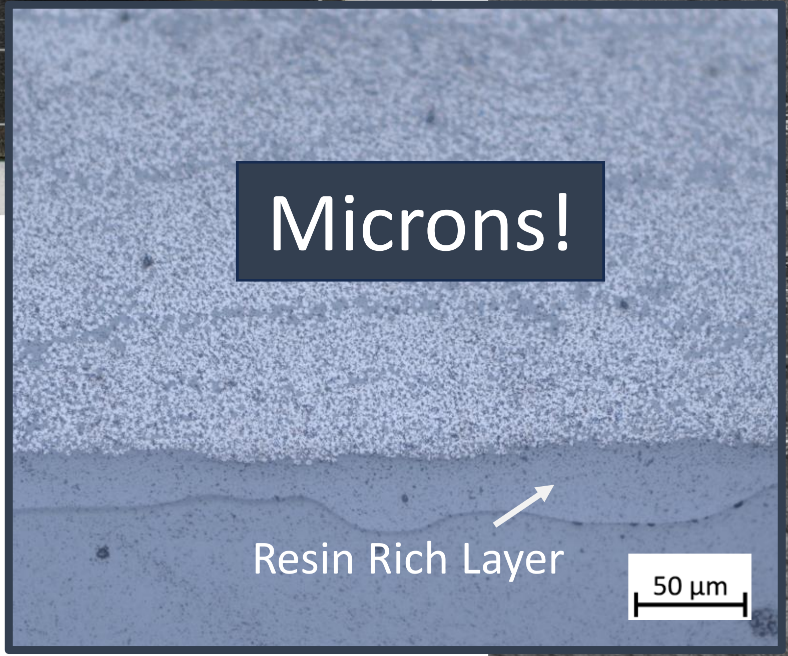

<u>Multidirectional laminates</u>

- CFRP $[0,45,-45,0,0,0]_S$
- CFRP $[0,0,0,45,-45,0]_S$

The resin plays a **<u>fundamental role in TSA</u>** and its effect must be addressed [2]

[2] Zhang D., Enke NF., Sandor BI. Thermographic stress analysis of composite materials. Experimental Mechanics.

MATERIAL: MULTIDIRECTIONAL CFRPs

Manufacturing was done in the autoclave following the manufacturers cycle

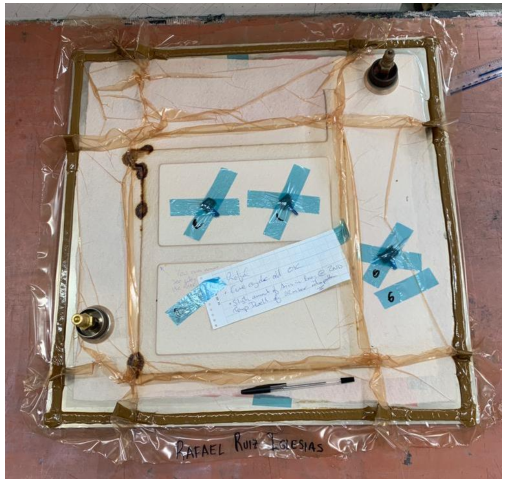

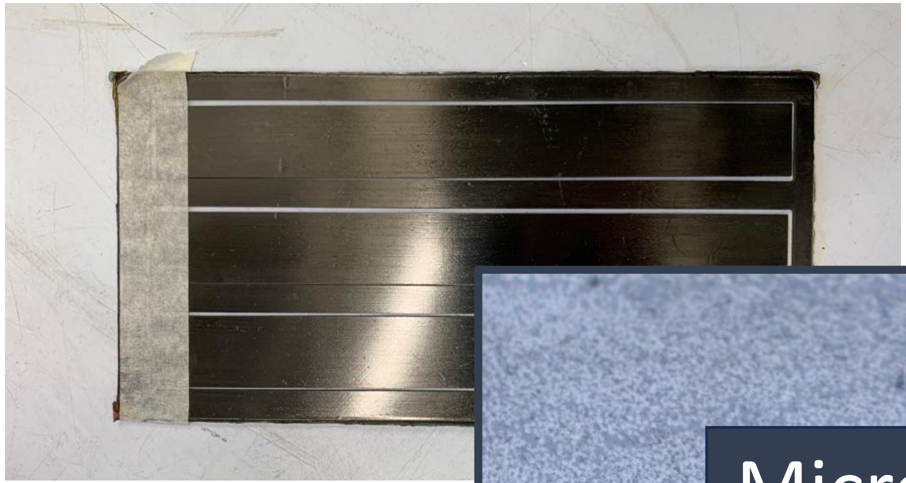

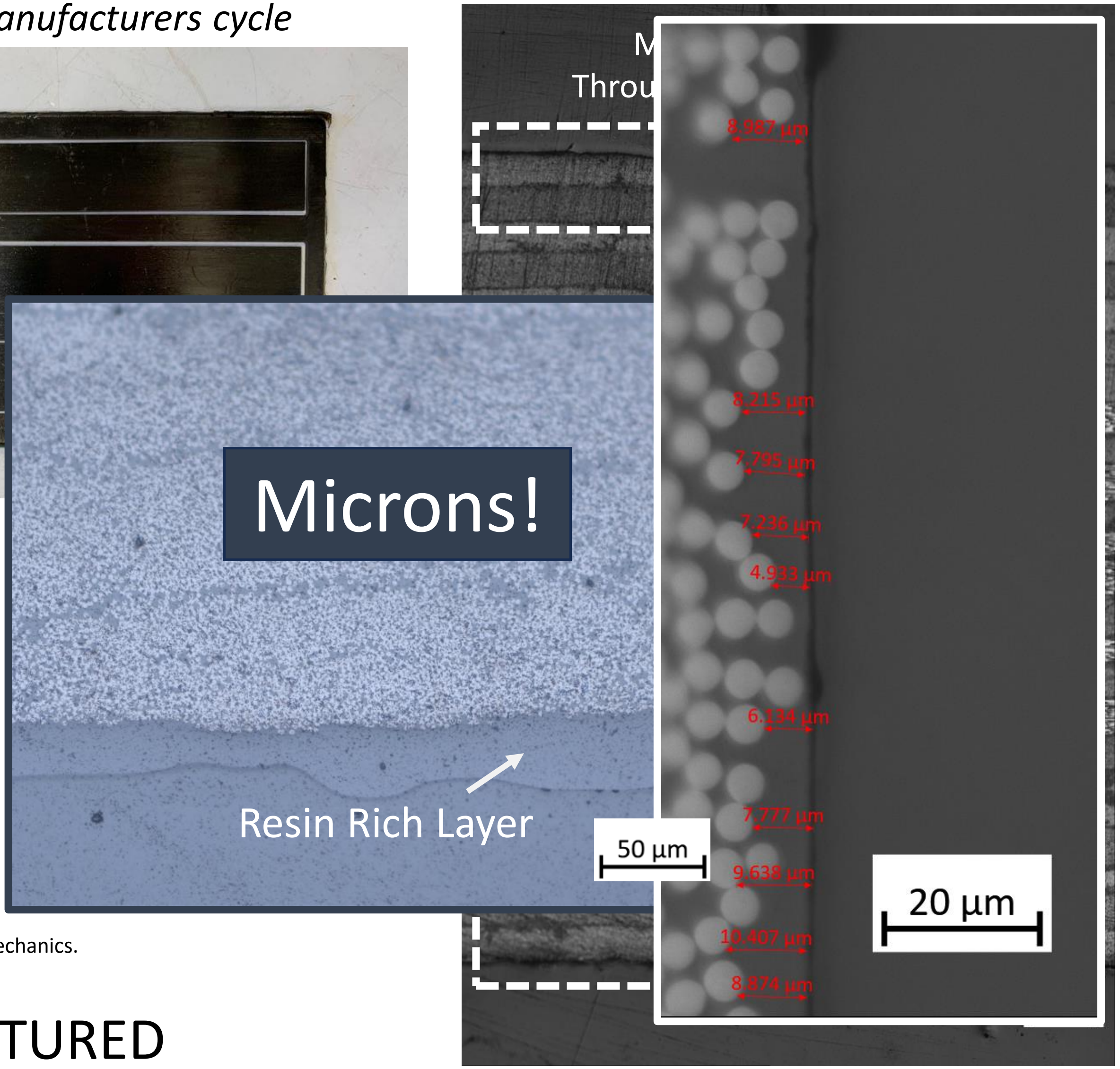

<u>Multidirectional laminates</u>

- CFRP $[0,45,-45,0,0,0]_S$
- CFRP $[0,0,0,45,-45,0]_S$

The resin plays a **<u>fundamental role in TSA</u>** and its effect must be addressed [2]

[2] Zhang D., Enke NF., Sandor BI. Thermographic stress analysis of composite materials. Experimental Mechanics.

2 SETS OF SPECIMENS WERE MANUFACTURED

MATERIAL: MULTIDIRECTIONAL CFRPs

$[0,45,-45,0,0,0]_S$

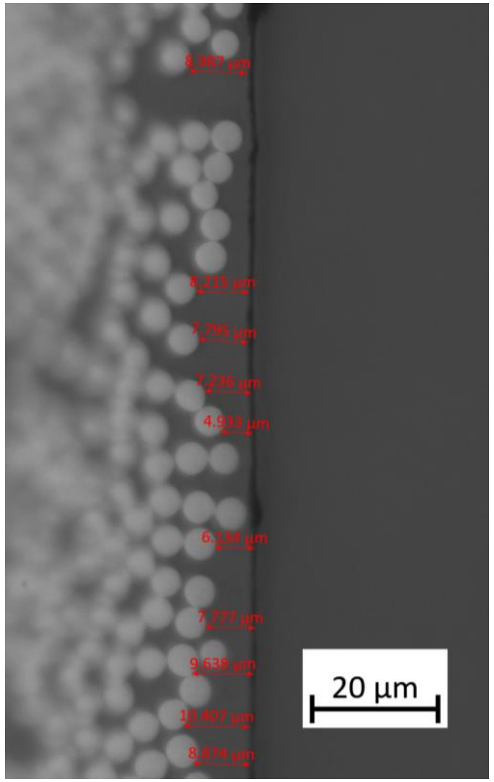

RRL thickness ≈ 8 µm

$[0,0,0,45,-45,0]_S$

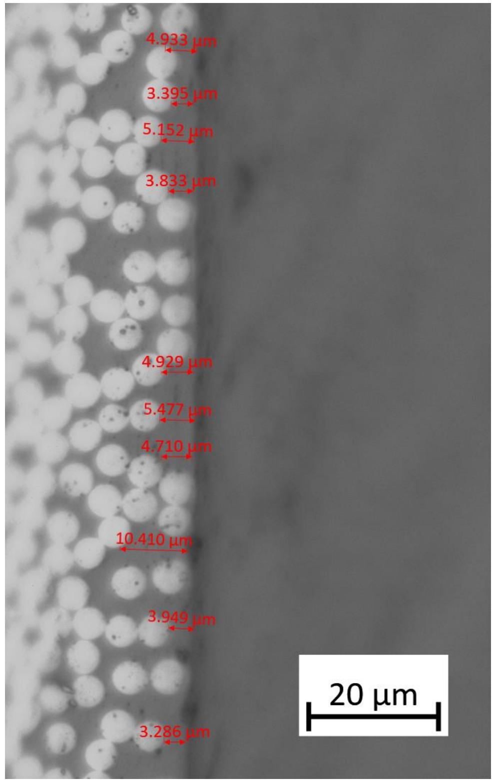

RRL thickness ≈ 5 µm

$[0,45,-45,0,0,0]_S$

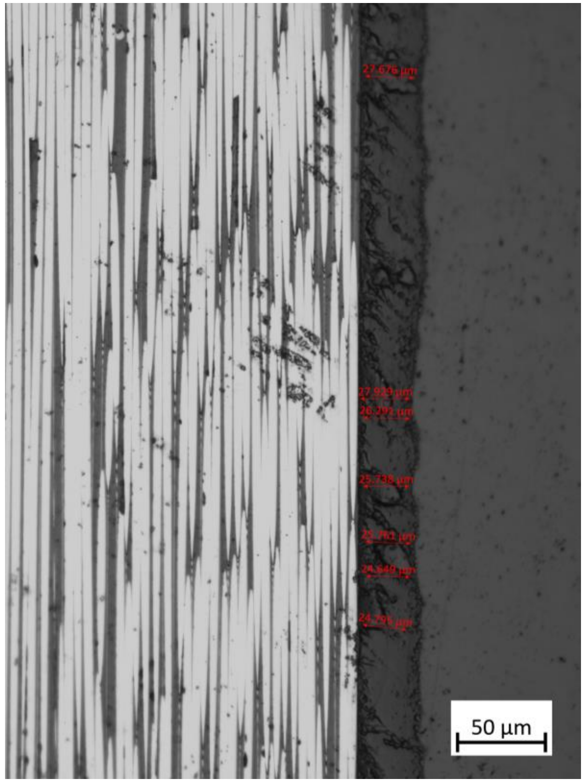

RRL thickness ≈ 25 µm

$[0,0,0,45,-45,0]_S$

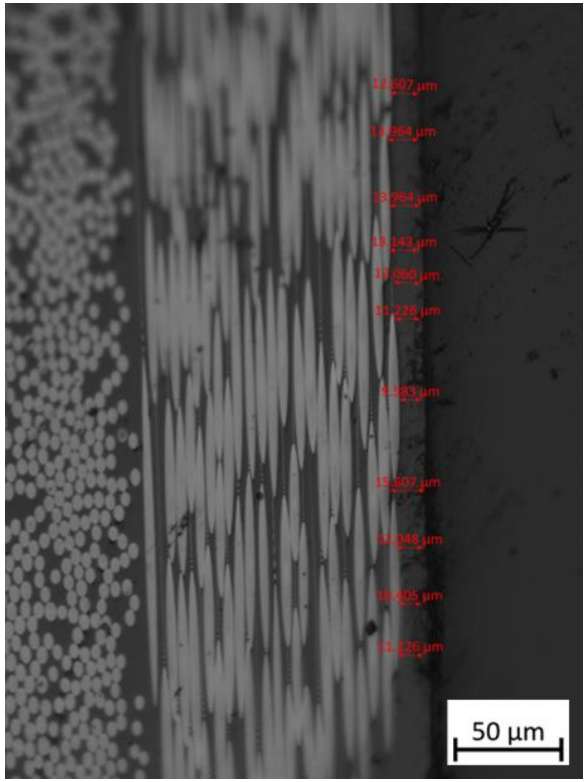

RRL thickness ≈ 12 µm

Thin resin rich surface layer

Thick resin rich surface layer

OH [0,45,-45,0,0,0]$_S$ TSA Results

Thin RRL (≈ 8 μm) OH specimen

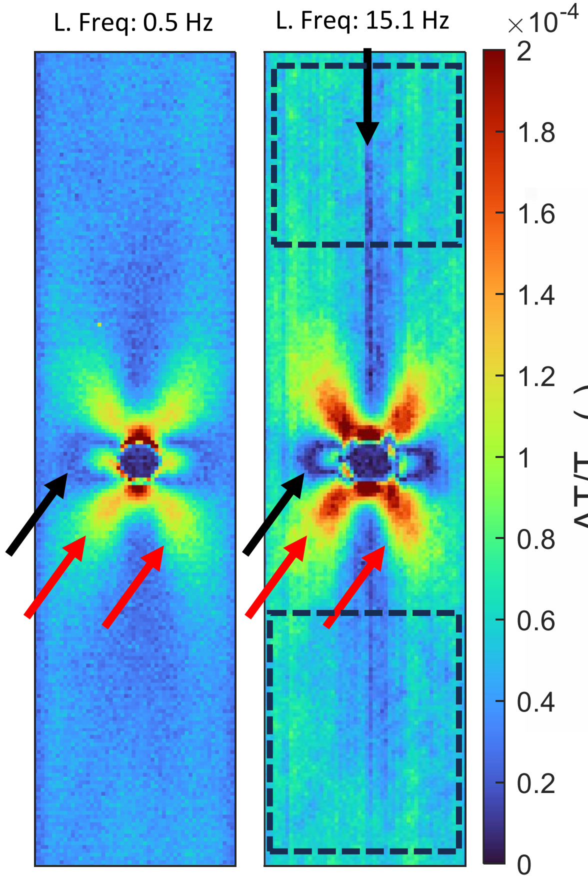

Animated GIF for the different frequencies

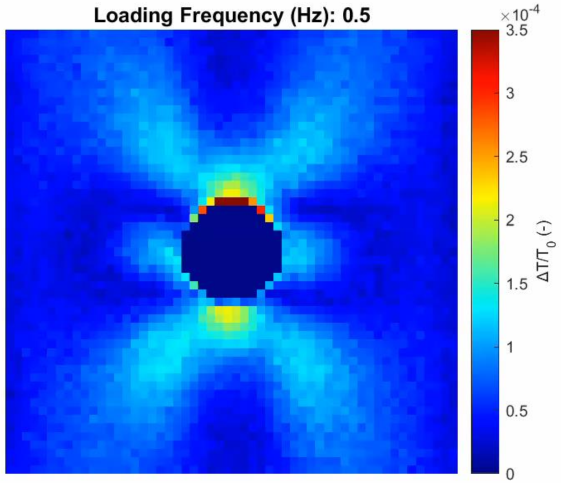

Symmetric at low frequencies **and asymmetric** response at high frequencies

Thick RRL (≈ 25 μm) OH specimen

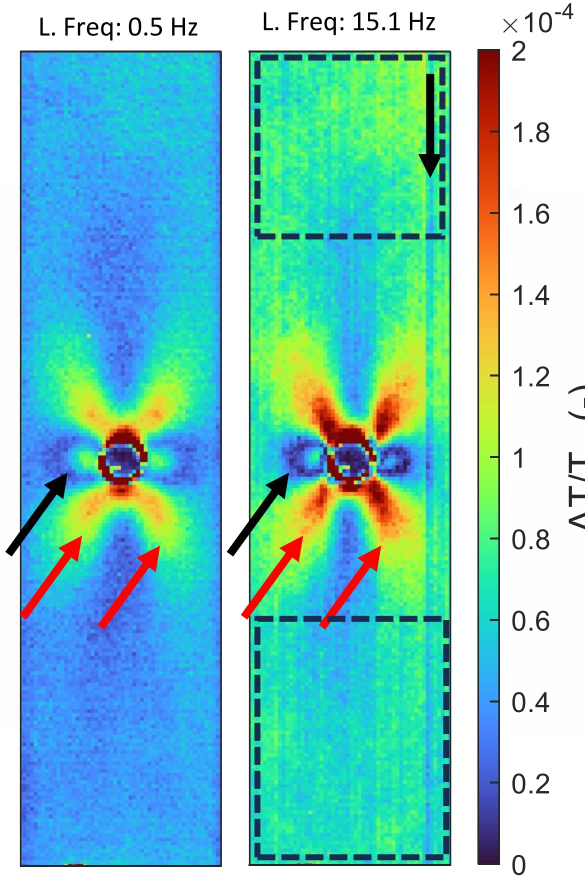

Animated GIF for the different frequencies

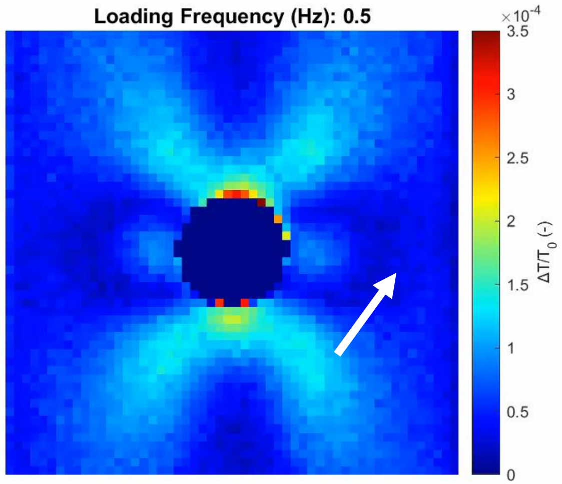

The *X* pattern is affected by the vertical feature

The thick RRL change in the thermoelastic response is more visible at 15.1 Hz

Different response pattern at different frequencies → *"X shape"*

The **observed pattern is a combination of the stress state from all the different plies** under different heat transfer conditions

OH $[0,0,0,45,-45,0]_S$ TSA Results

Thin RRL (≈ 5 μm) OH specimen

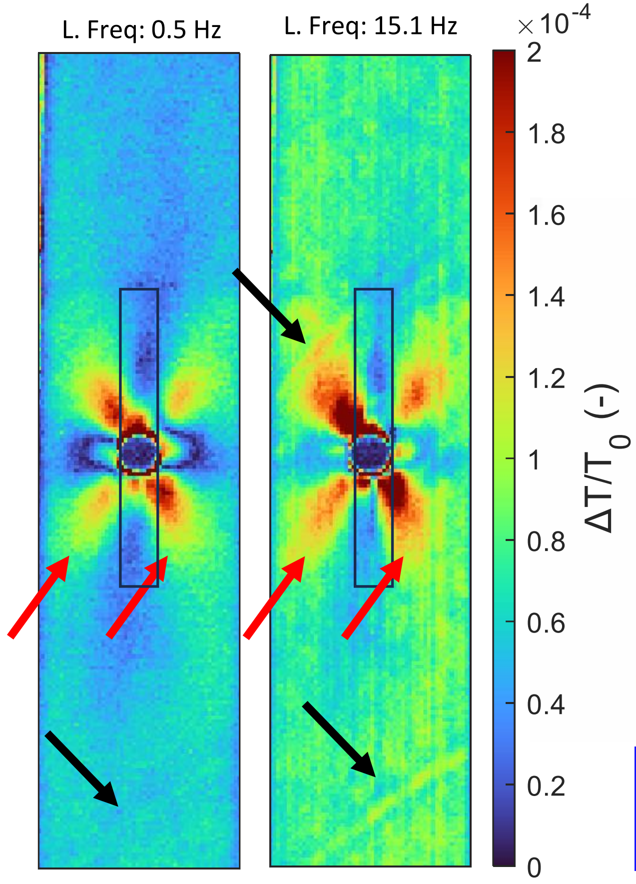

Animated GIF for the different frequencies

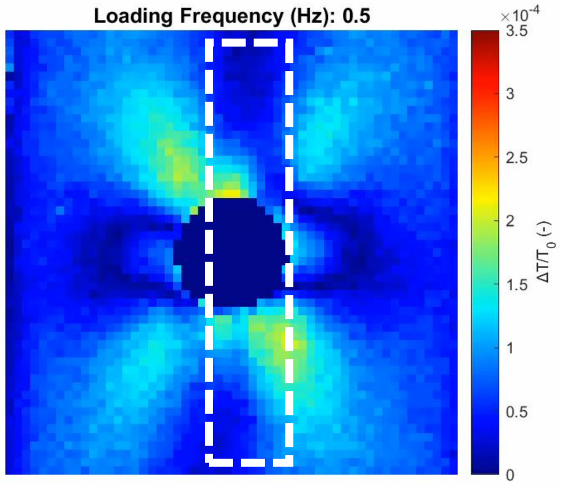

The fibres removed are more visible as frequency is increased

Thick RRL (≈ 12 μm) OH specimen

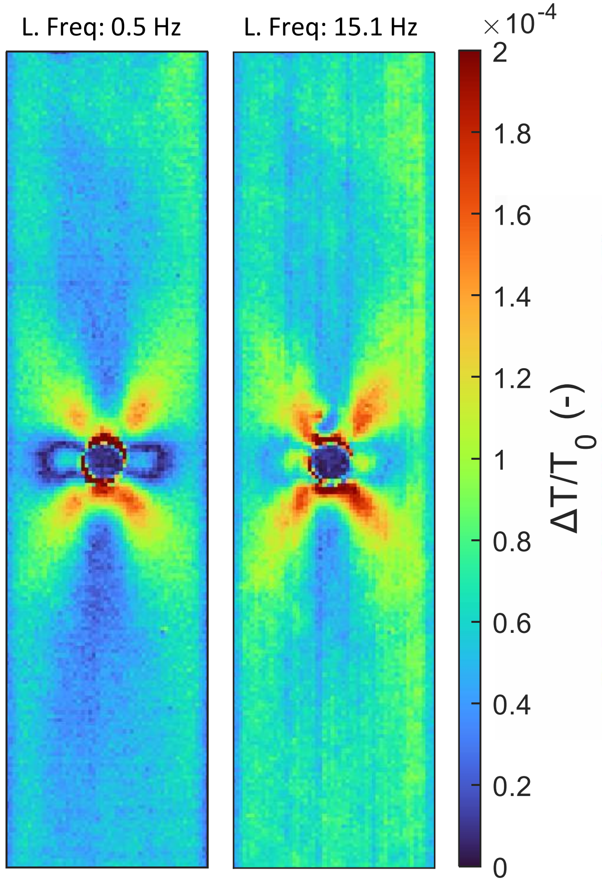

Animated GIF for the different frequencies

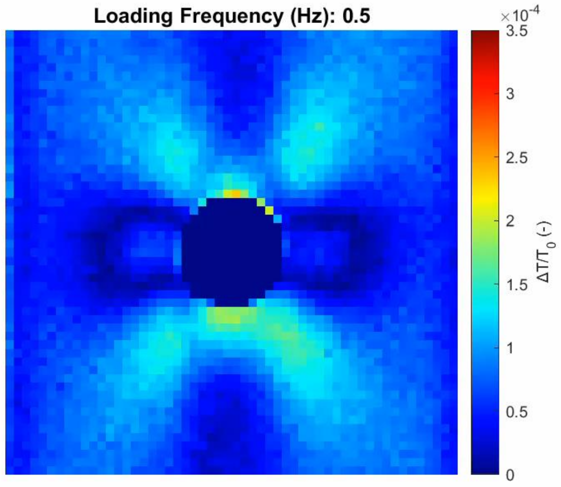

Behaviour without any damage being induced

Fibre removed when drilling the hole!

Some damage can be induced in real structures // Wrinkles are also found in the sample with the thin RRL (More visible at higher frequencies)

These unexpected features **change the response pattern!**

DIC Results - STRAIN ANALYSIS

Thin Resin $[0,45,-45,0,0,0]_S$

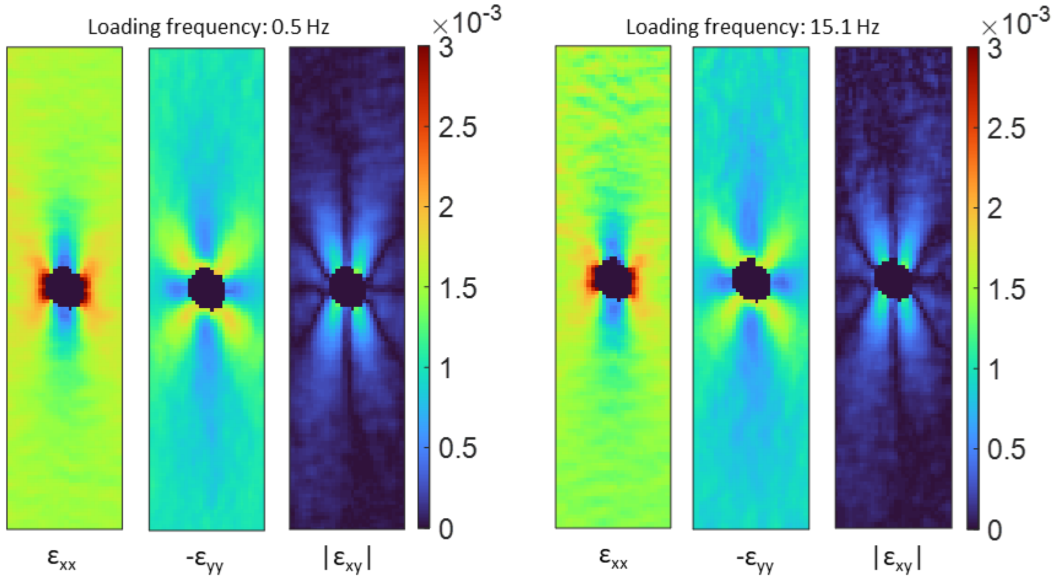

Thin Resin $[0,0,0,45,-45,0]_S$

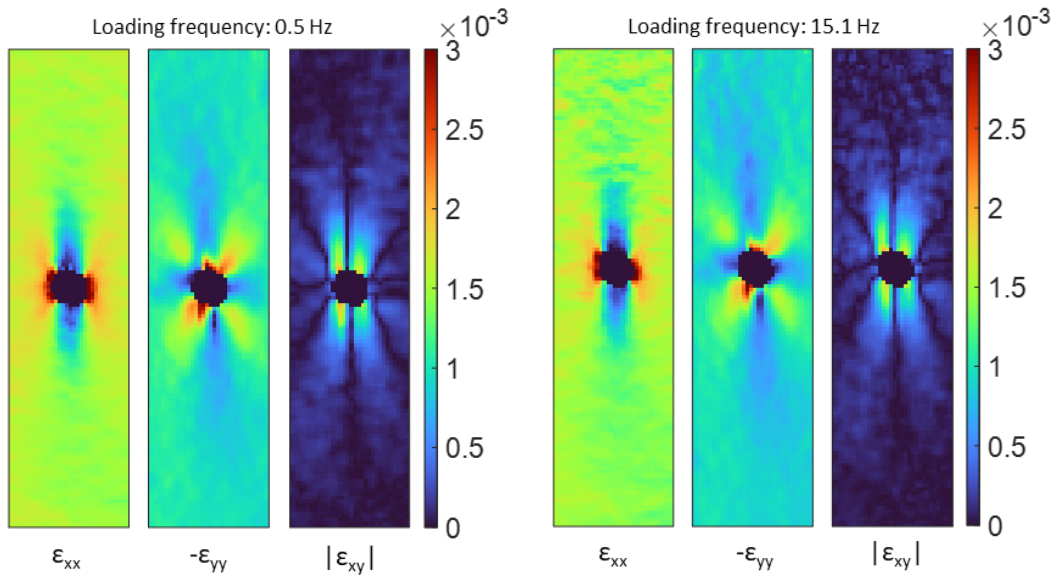

- **Strain results are consistent at 15.1 Hz**
- **Fibre bundle removed** when drilling the hole of $\mathbf{[0,0,0,45,-45,0]_S}$ → Stress / Strain redistribution
- The next step is to compare the experimental with an FEA simulation done in ABAQUS
- Excellent strain agreement

Although some differences can be observed → DIC uncertainties (e.g. spatial filtering)

DIC Results - STRAIN ANALYSIS

Thin Resin $[0,45,-45,0,0,0]_S$

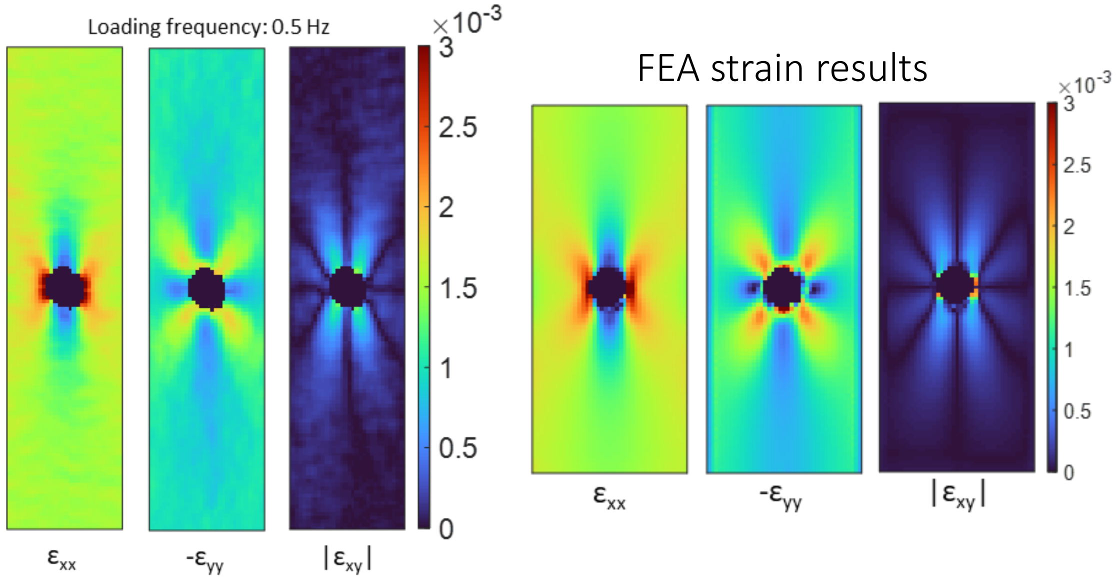

Thin Resin $[0,0,0,45,-45,0]_S$

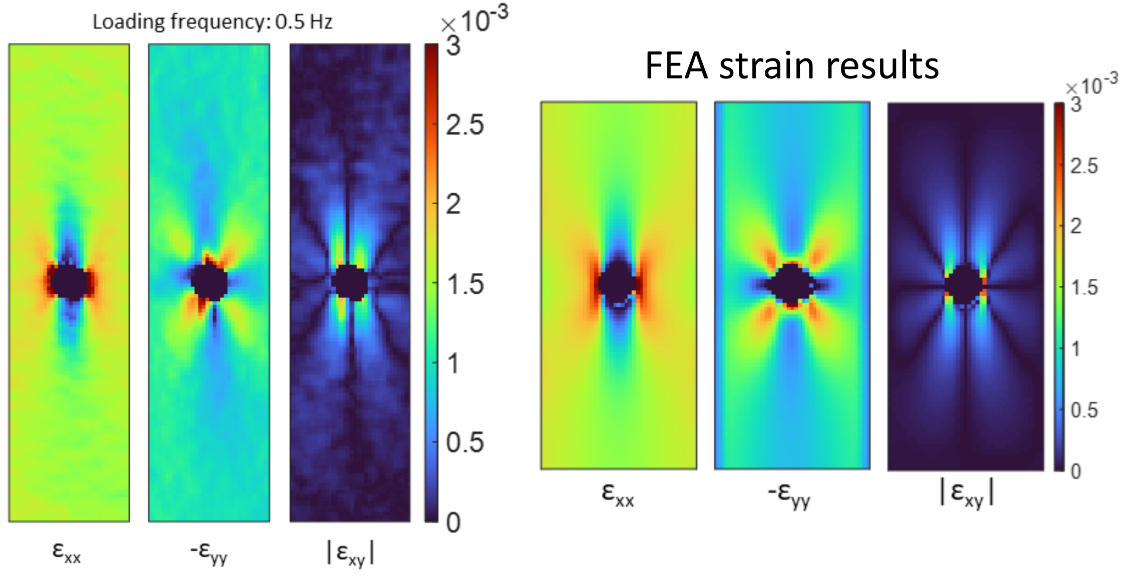

- **Strain results are consistent at 15.1 Hz**
- **Fibre bundle removed** when drilling the hole of $\mathbf{[0,0,0,45,-45,0]_S}$ → Stress / Strain redistribution
- The next step is to compare the experimental with an FEA simulation done in ABAQUS
- Excellent strain agreement

Although some differences can be observed → DIC uncertainties (e.g. spatial filtering)

HYBRID APROACH FULL FIELD DATA INTEGRATION

HYBRID APROACH FULL FIELD DATA INTEGRATION

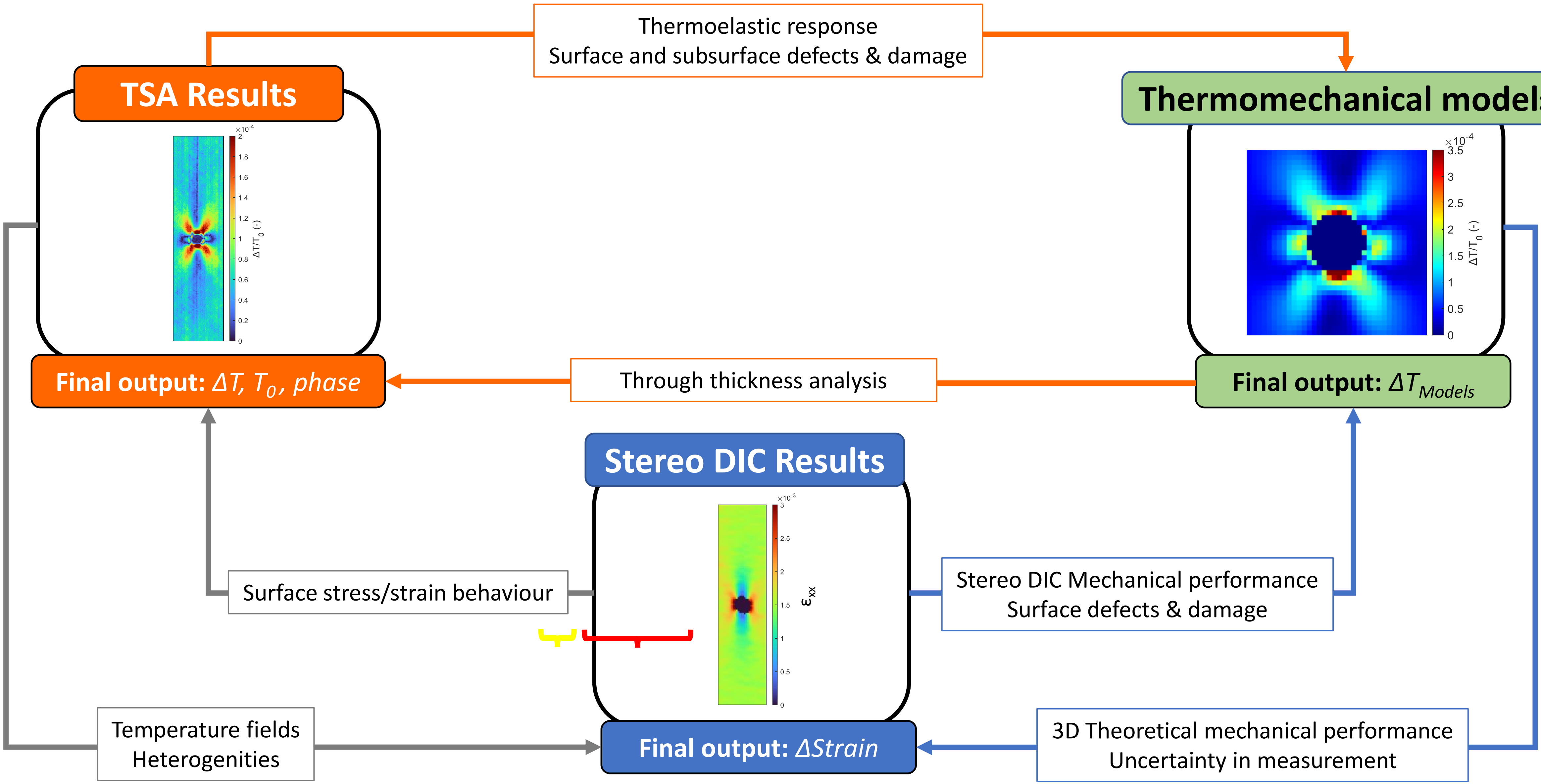

HYBRID APROACH FULL FIELD DATA INTEGRATION

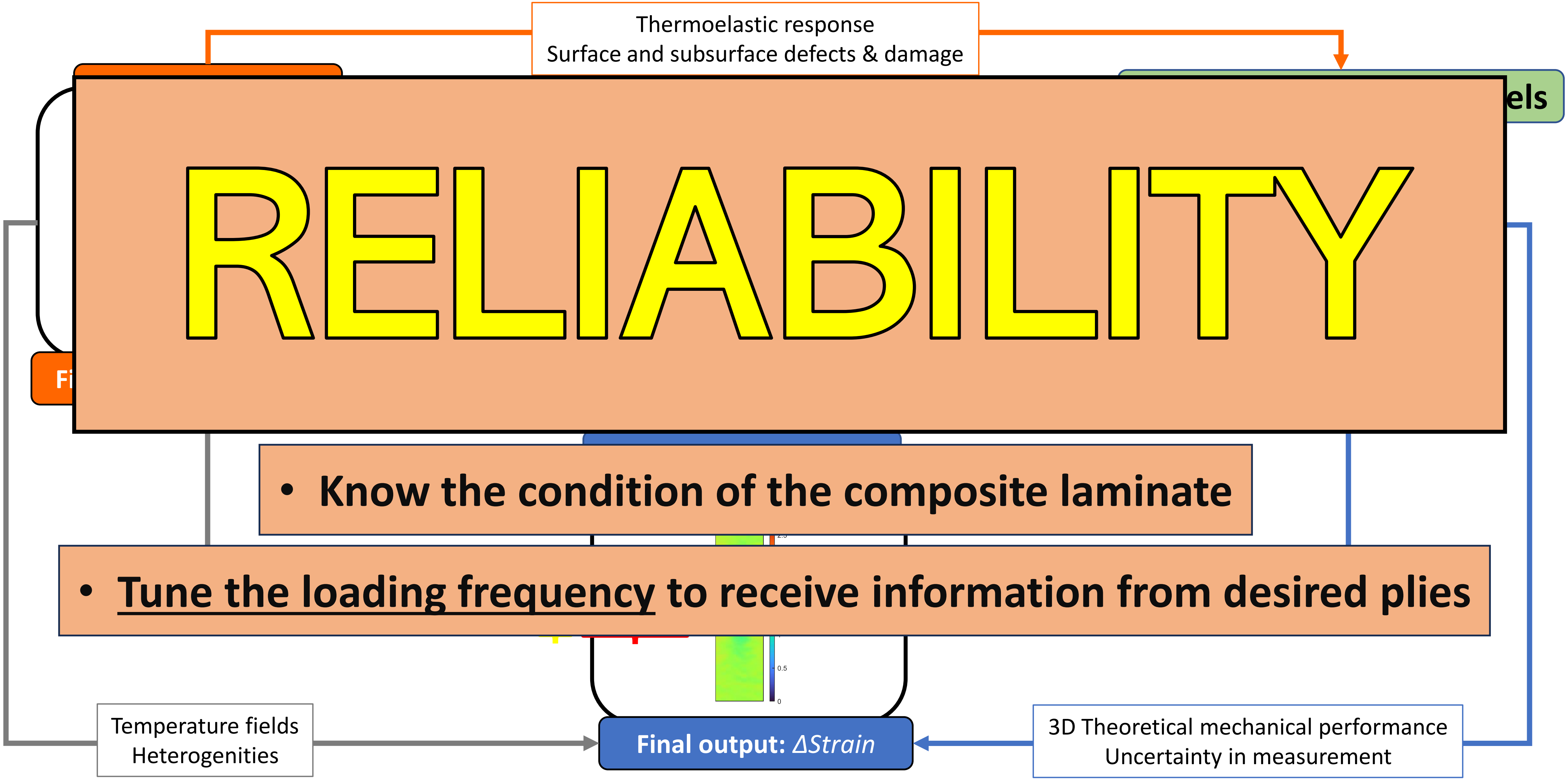

THERMOMECHANICAL MODELS

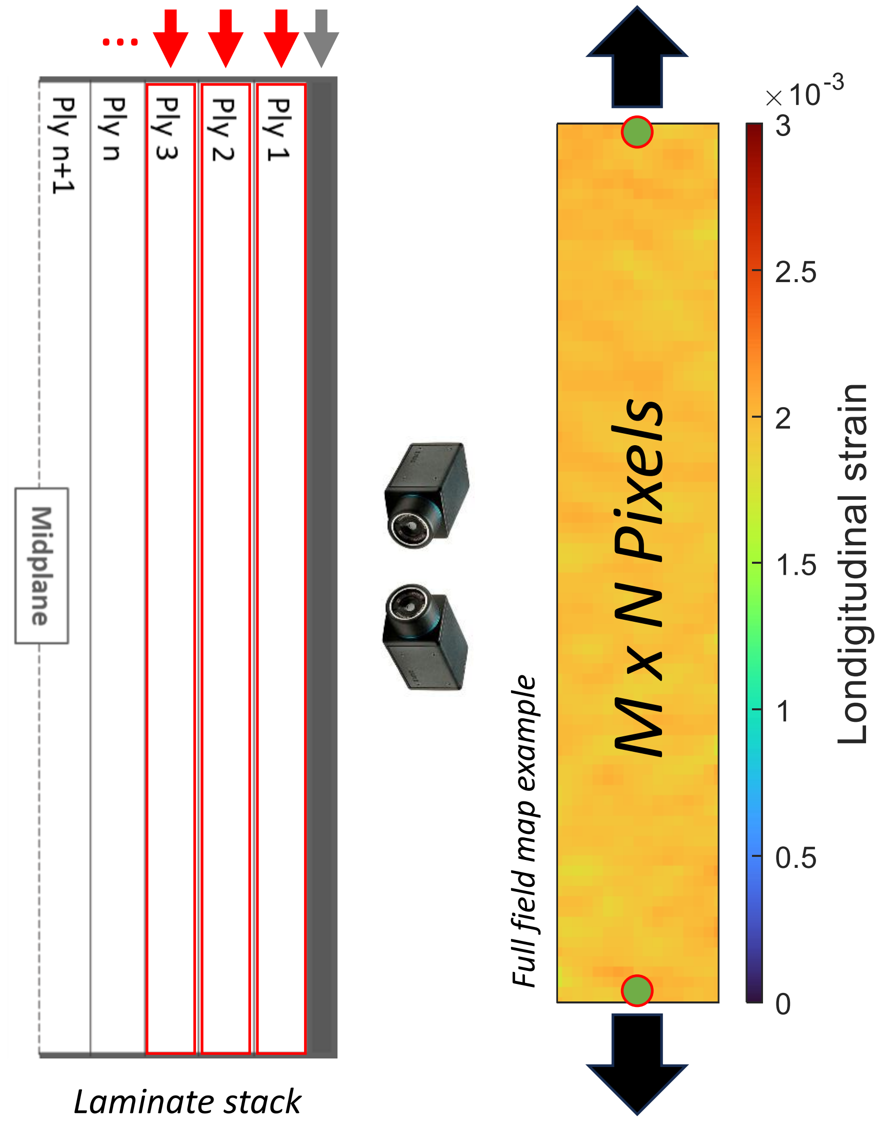

Experimental models *// Mathematical (Dimensions: M x N)*

Resin Response: Full field $\Delta\varepsilon_{DIC}$ → ΔT_{RRL}

ΔT is generated by the strain experienced by the resin layer

Individual Ply Response: Full field $\Delta\varepsilon_{DIC}$ → $\Delta T_{I.Ply}$

ΔT is generated by a single ply and is a function of the ply properties

These experimental **strain models** are always **independent of heat transfer**

Finite Element Analysis (FEA) model *(Dimensions: Defined by user)*

Non-Adiabatic FEA Model [3]: Full field $\Delta\varepsilon_{FEA}$ → ΔT_{FEA}

ΔT is calculated using a parametric thermomechanical model developed in Abaqus (Considers RRL effects and conduction between plies)

**Far field displacement calibration*

This model allows the user to **obtain ΔT at any desired loading frequency**

[3] Cappello R., Pitarresi G., Catalanotti G. Thermoelastic Stress Analysis for composite laminates: A numerical investigation. Composites Science and Technology. 2023; 241: 110103.

ISOLATED PLIES $\Delta T/T_0$ - Thermomechanical Models

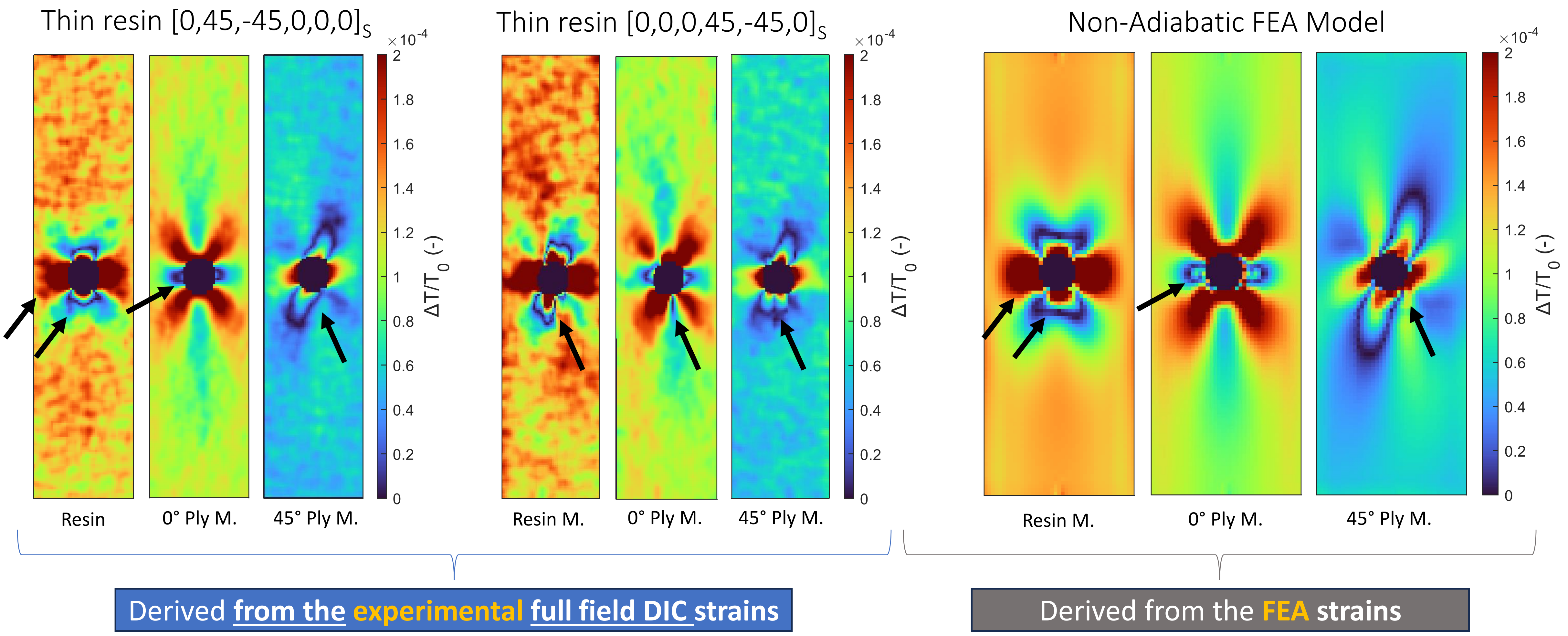

- Good correlation between the intact $[0,45,-45,0,0,0]_S$ and FEA results

Some differences → DIC uncertainties

**Spatial filtering*

- Defects (e.g. fibre pullout) change the thermoelastic "shape" which the FEA model doesn't account for

Through thickness TSA analysis (FEA Model)

Thin resin OH $[0,45,-45,0,0,0]_S$

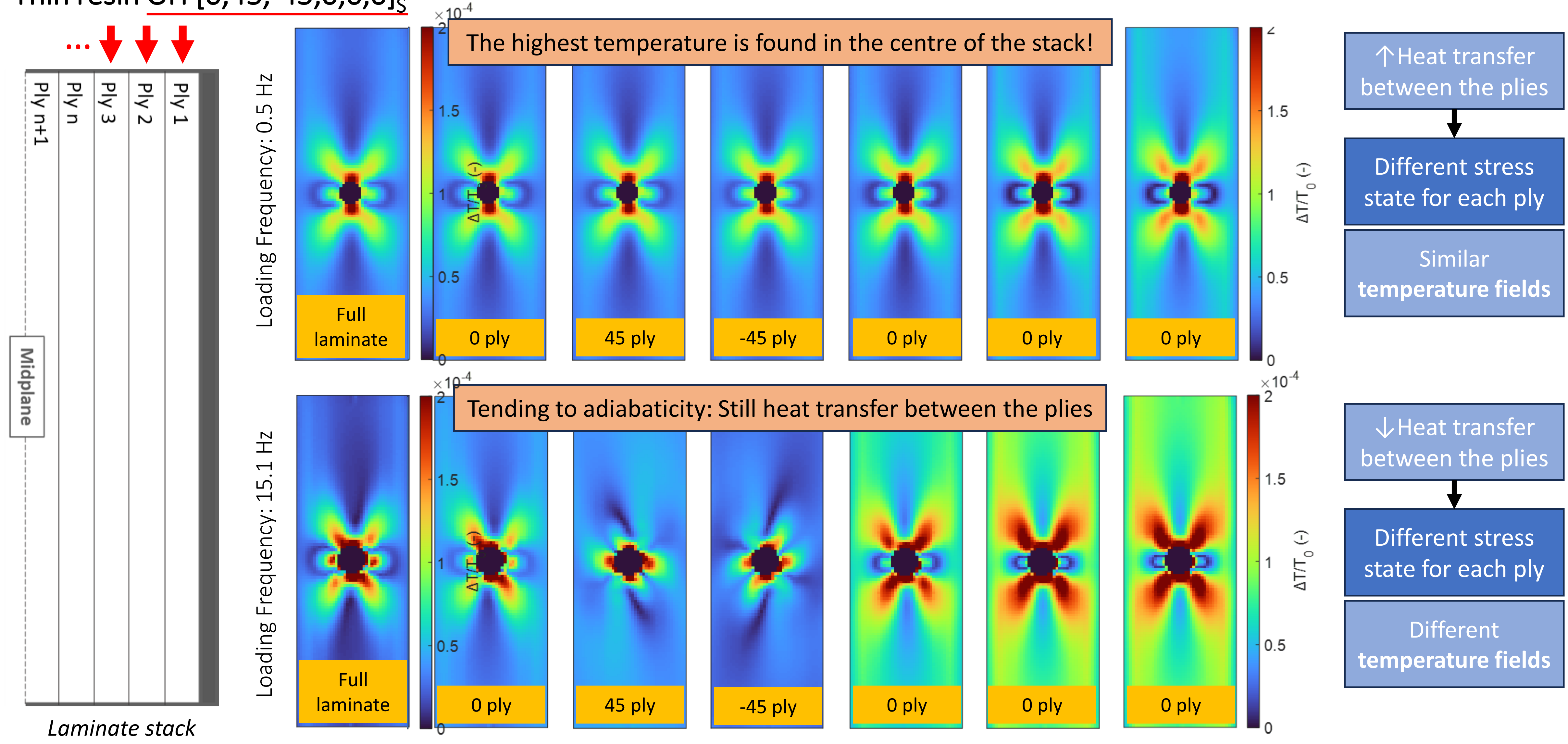

CONCLUSIONS → Reliability in the measurement

- A **<u>FAST, IN SITU, NEW APPROACH</u>** has been demonstrated based on integrating **TSA + DIC** results **+ TSA Modelling**
- The **model was validated** under 3D stress states.
- **DIC data analysis and filtering influence** the full field strain derived ΔT models.
- Manufacturing/machining **defects modify the thermoelastic response** due to stress redistribution → **Can be located!**
- **A through thickness analysis** of the ΔT can be performed **using the thermomechanical FEA model** → Tune loading freq.

FURTHER WORK

- **Influence of material properties in the analysis**

  18. Thermography-based Nondestructive Evaluation (NDE), Process Monitoring, Data Fusion– Monday 3rd (5:10 PM–5:30 PM)
  A tool to obtain the coefficients of thermal expansion for CFRP composites using full-field data fusion #17536
- **Different and realistic loading scenarios** where the strain is not uniform through the thickness of the laminate
- Effect of the matt black **paint on TSA** results.

EXPERIMENTAL SETUP / Pictures

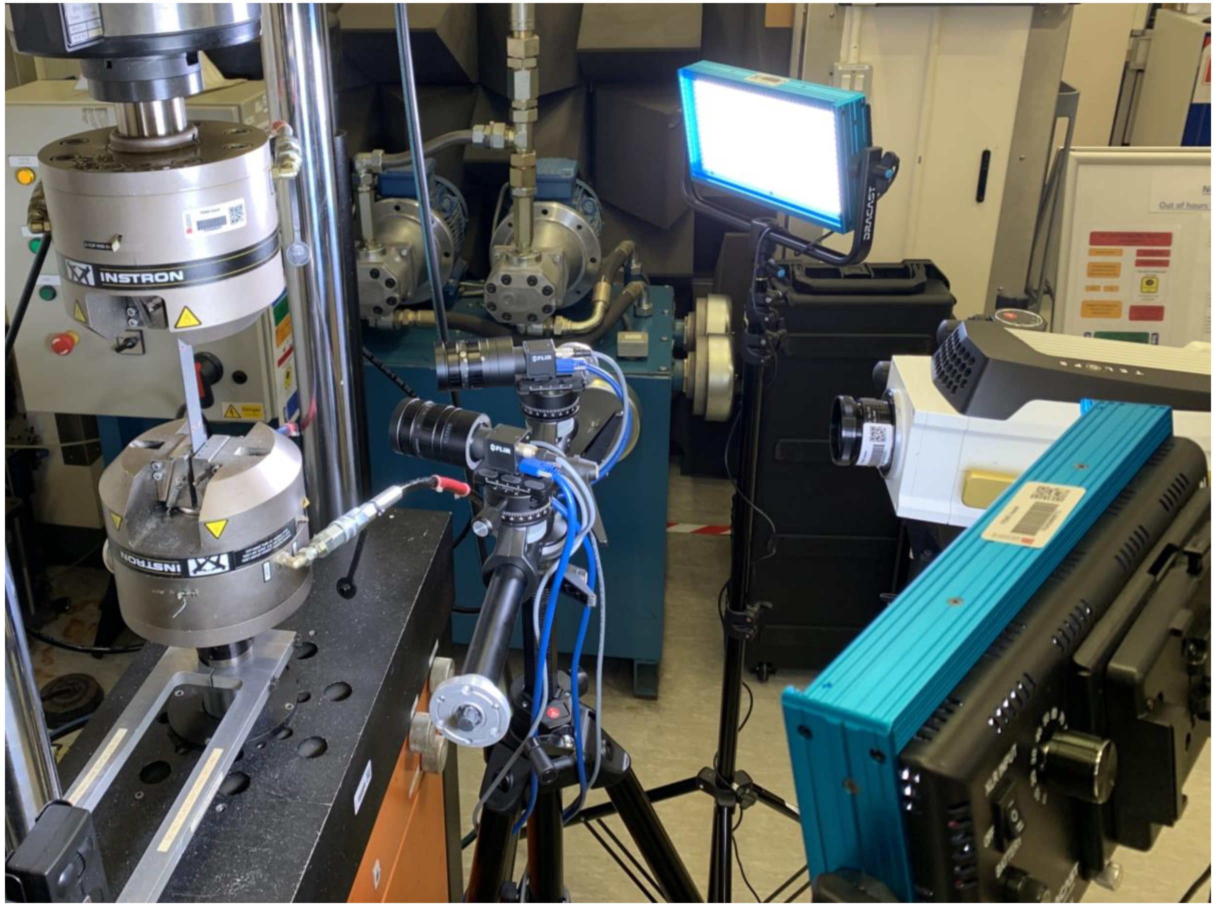

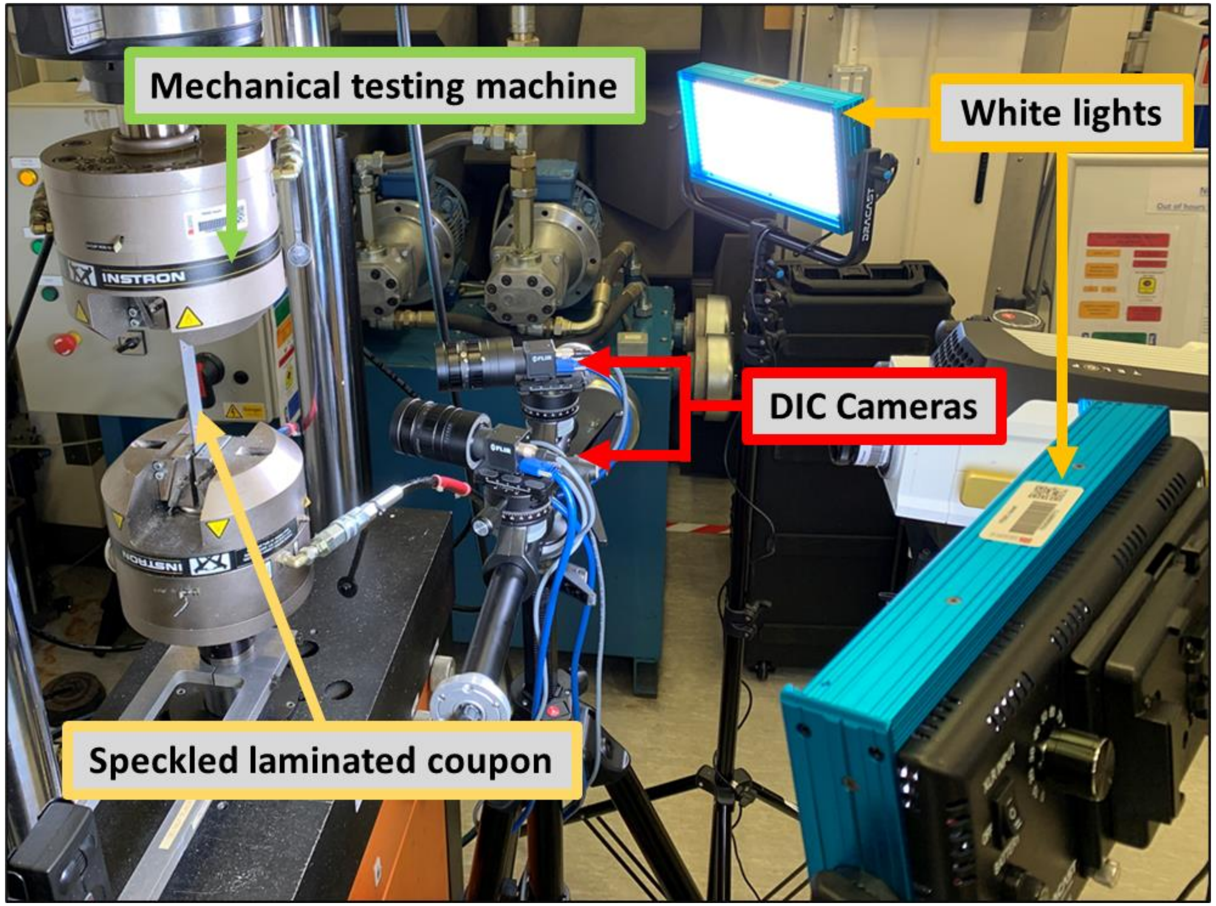

PAINT EFFECT ON TSA

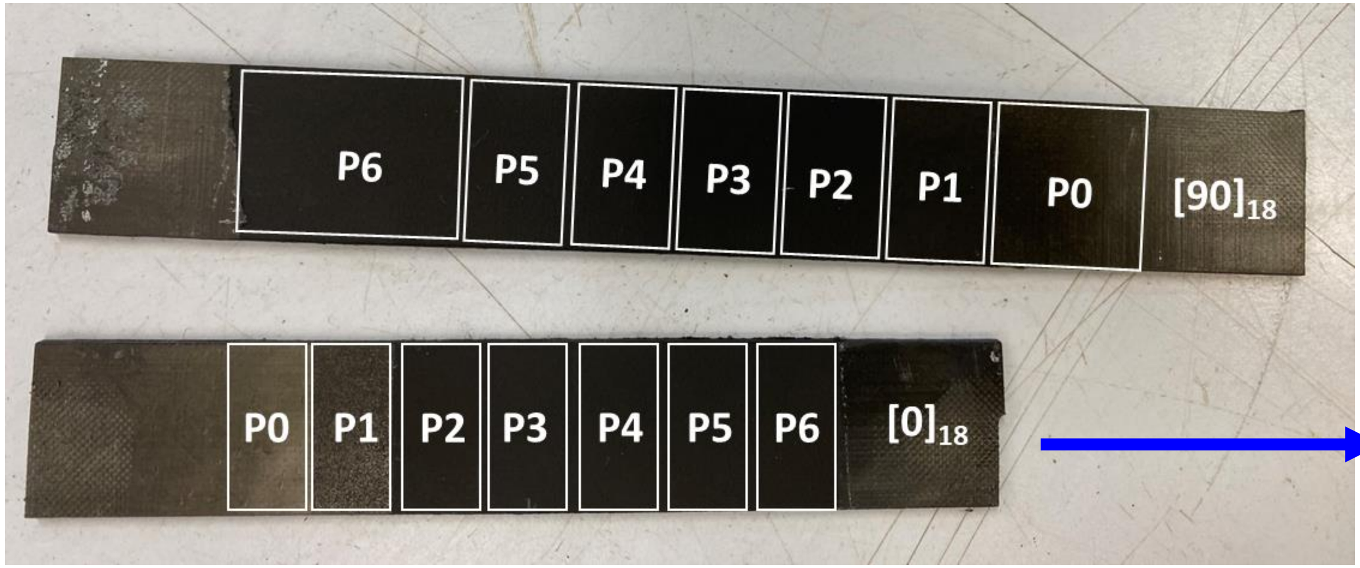

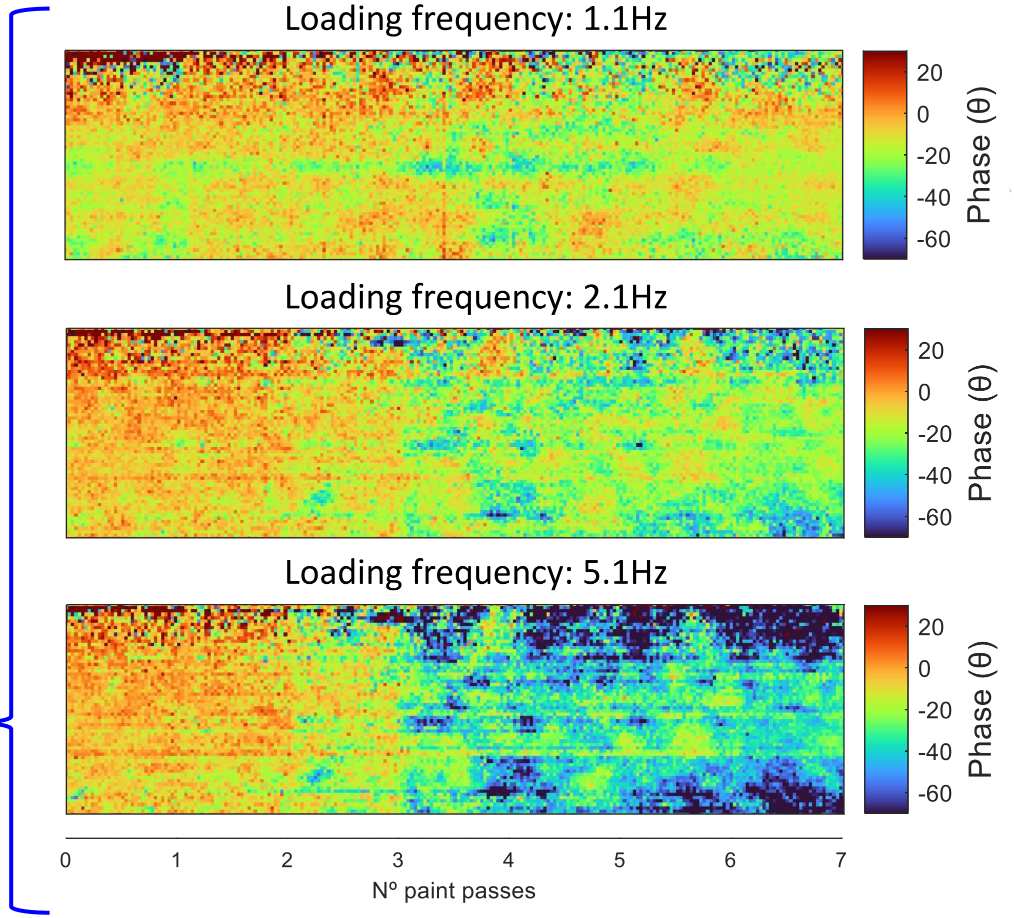

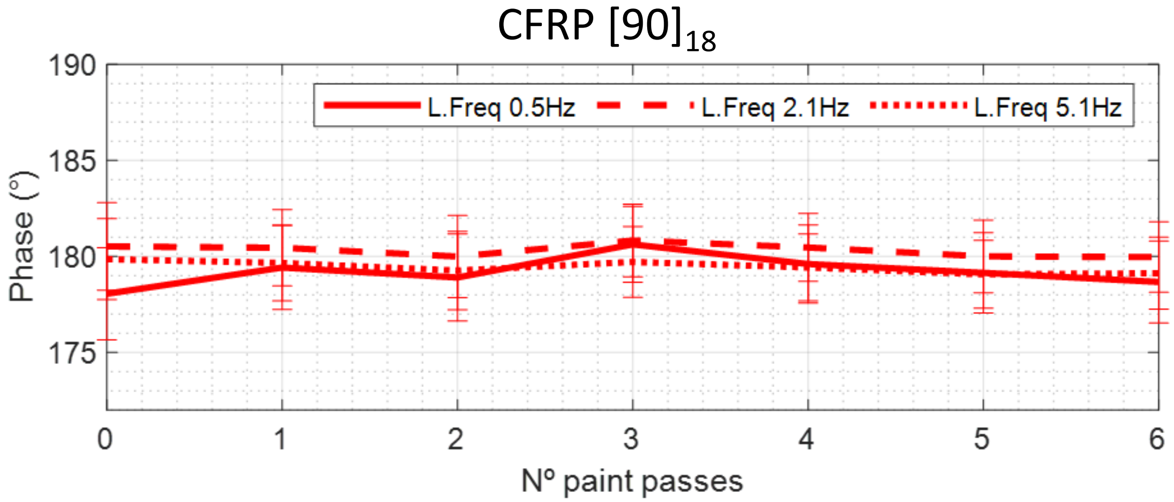

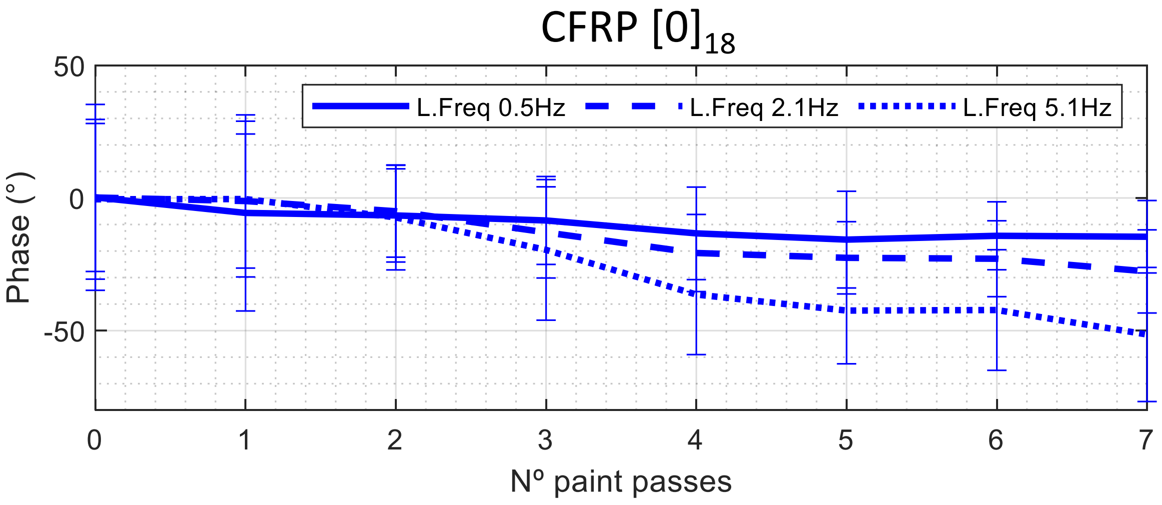

OTHER TESTS / C-Spar

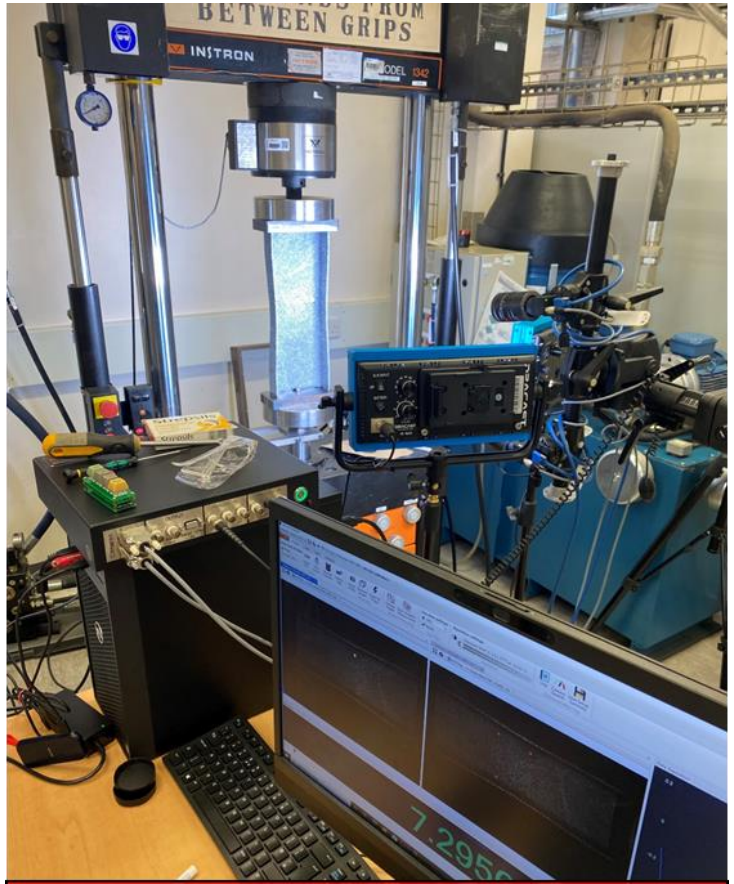

Speckled C-Spar

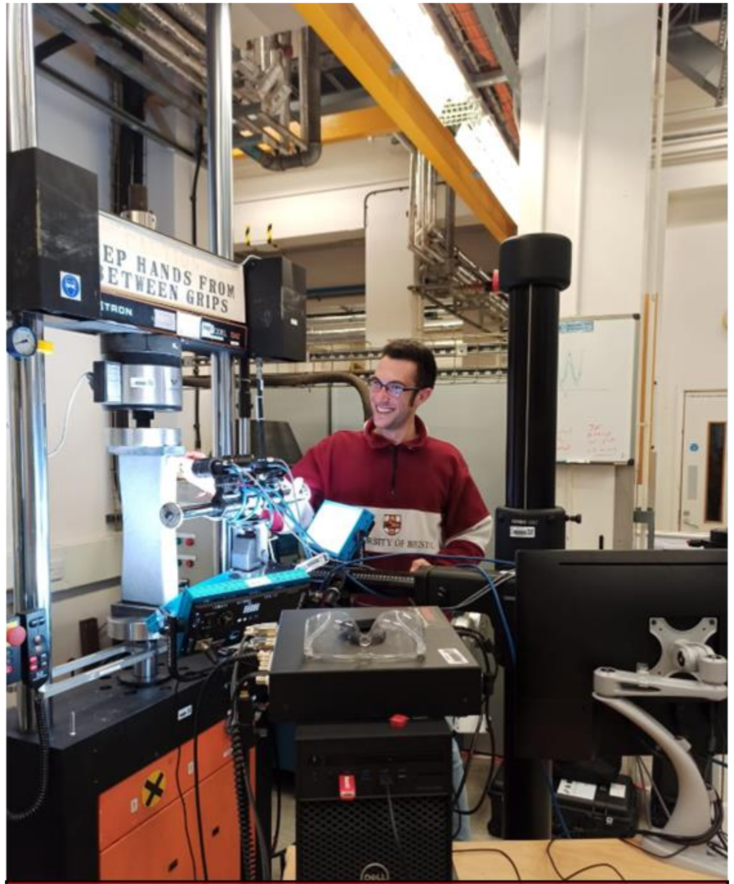

Rafa calibrating the tests

Rafa before breaking the C-Spar

IM7/8552 Properties and Data Processing

IM7/8552 mechanical and thermal properties.

Property	Value
Young's modulus E_1 (GPa)	159.533
Young's modulus E_2 (GPa)	10.121
Poisson's ratio v_{12}	0.325
Shear modulus G_{12} (GPa)	5.138
Thermal expansion coeff. α_1 (10^{-6} K-1)	**-0.102**
Thermal expansion coeff. α_2 (10^{-6} K-1)	**23.138**
Density ρ (kg/m^3)	1569.2
Specific heat capacity Cp (J kg^{-1} K^{-1})	884.53

Monday 5:10 PM Hemlock/Oak

TSA parameters.

Technique used	Thermal Image Acquisition
Infrared fast camera	Telops Fast M3K
Lens	50 mm
Camera resolution	≈ 20 mK
Pixel to mm conversion	1 px = 0.31 mm
Frames	5250
Frame Rate	383 Hz

DIC parameters and evaluation for testing the unnotched specimens.

Technique used	3D / Stereo Digital Image Correlation	
	Camera 1 (Blackfly-12.3 MPx)	Camera 2 (Blackfly-12.3 MPx)
Sensor, digitalization	Sony IMX226 (CMOS) , 4096 x 3000	
Stereo angle	19.53°	
Frame rate	10 Hz	
Camera noise (% of range)	0.454%	0.443%
Lens and imaging distance	25 mm	25 mm
Total number of images	316	316
DIC software package	MatchID	
Pixel to mm conversion	1 px = 0.0876mm	
ROI (mm)	112.8 x 24.49	
Coordinate transformation	Best-plane-Fit	
Subset, step	13, 10	
Interpolation, shape function, correlation	Bicubic, Quadratic, ZNSSD	
Pre-smoothing	Gaussian Smoothing	
Displacement resolution	$2.176 \cdot 10^{-3}$ mm	
Strain conversion	Log. Euler–Almansi	
Smoothing technique	Local polynomial - affine least-squares fit	
Strain window (pixels)	15 data points	
VSG	153 pixels	
Strain resolution	0.00790%	

HOW IS HEAT TRANSFER OCURRING?

TSA is based on the thermoelastic effect, which describes the coupling between mechanical deformation and thermal energy in an elastic solid and was established by Lord Kelvin (W. Thomson) [4] in 1855

Change in T is proportional to the change of the sum in the principal stresses under adiabatic conditions, and is loaded within the elastic region of the material

$$\dot{T} = \frac{T_0}{\rho C_\varepsilon}\frac{\partial \sigma_{ij}}{\partial T}\dot{\varepsilon}_{ij} - \frac{\dot{Q}}{\rho C_\varepsilon} \text{ for } i,j = 1,2,3$$

$$\dot{Q} = k\nabla^2 T$$

If $\dot{Q}$ (rate of internal heat generation) = 0 → Adiabatic

To minimise the effect of $\dot{Q}$ (internal heat generation) an **increase in the <u>loading frequency</u>** is required → Increase in $\dot{\varepsilon}_{ij}$

→ The $\dot{Q}$ term can be neglected

The thermal diffusion length decrease, and "*pseudo*" adiabatic conditions are achieved

[4] W. Thomson (Lord Kelvin): On dynamical theory of heat, Trans. R. Soc. Edinburgh 20, 261–283 (1853)

IM7/8552 COUPONS MANUFACTURING

- Manufactured in an **autoclave following the manufacturer recommended curing cycles.**

- All panels were made either with peel ply or caul plate: for the peel ply each side of the panels has either a ‘smooth’ surface, which was in contact with the aluminum mold, or a rough surface containing the characteristic peel ply imprint.

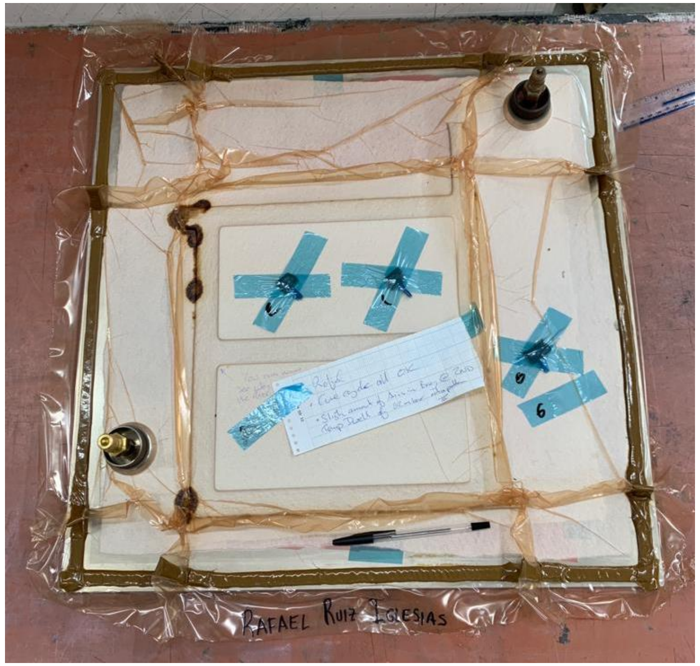

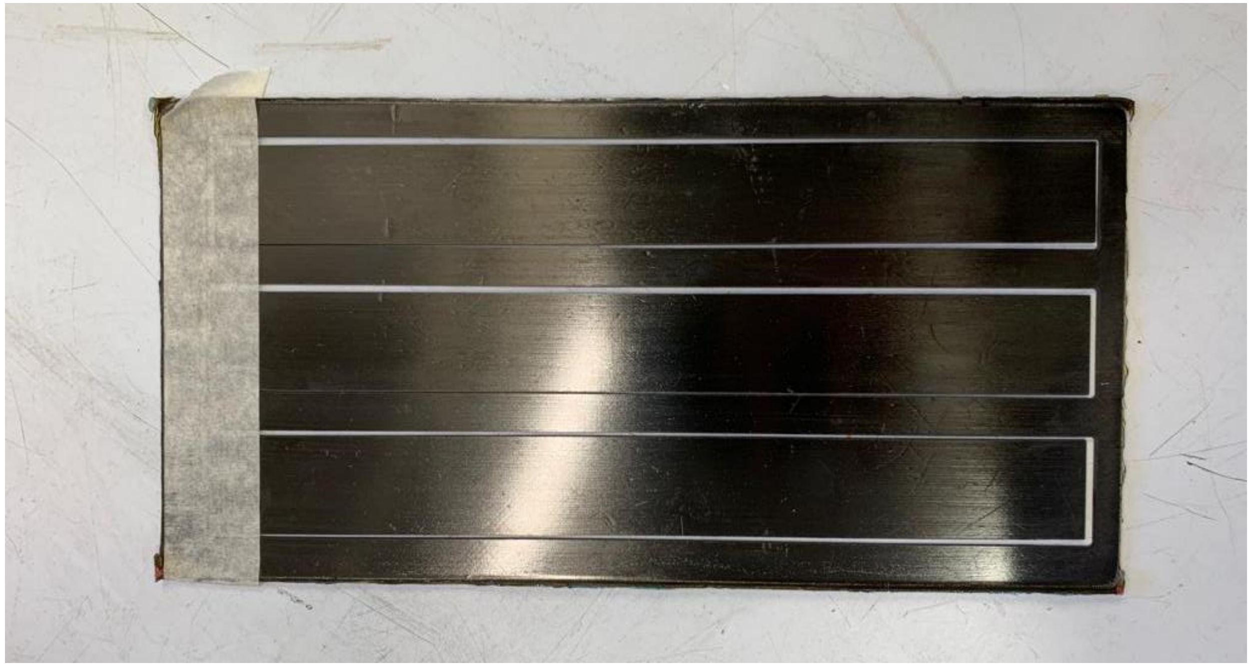

ALL IM7/8552 Properties

Layups	$[0, 0, 0, 45, -45, 0]_s$, $[0, 45, -45, 0, 0, 0]_s$
Loading frequencies (Hz)	0.5, 1.1, 2.1, 3.1, 4.1, 5.1, 6.1,7.1,8.1,9.1,10.1,12.1, 15.1, 17.1, 20.1, 22.1, 25.1, 27.1, 30.1
Ply thickness (mm)	0.125
Number of loading cycles	3
Resin layer thickness (μm)	(5, 12), (8, 25)
Experimental sampling frequency (Hz)	383.0
Numerical sampling	50 points per cycle

Property	IM7/8552
Young's modulus E_1 (GPa)	159.5*
Young's modulus E_2 (GPa)	10.1*
Poisson's ratio ν_{12}	0.325*
Shear modulus G_{12} (GPa)	5.14*
Thermal expansion coeff. α_1 (10^{-6} K^{-1})	-0.102*
Thermal expansion coeff. α_2 (10^{-6} K^{-1})	23.138*
Thermal conductivity k_1 (W m K^{-1})	5
Thermal conductivity k_2 (W m K^{-1})	0.6
Density ρ (Kg dm^{-3})	1.5692*
Specific heat C_ε (J Kg^{-1} K^{-1})	884.53

Property	Epoxy resin
Young's modulus E (GPa)	3.8
Poisson's ratio ν	0.35
Shear modulus G_{12} (GPa)	2.71
Thermal expansion coeff. αr (10^{-6} K^{-1})	53.5
Thermal conductivity k (W m K^{-1})	0.2
Density ρ (Kg dm^{-3})	1.153
Specific heat C_ε (J Kg^{-1} K^{-1})	1110

DIGITAL IMAGE CORRELATION

DIC tracks changes in contrast to obtain **displacements** and hence calculate **surface strain fields (Δε)**

- Full field
- White light imaging technique

***DIC** Cameras: Surface Displacements*

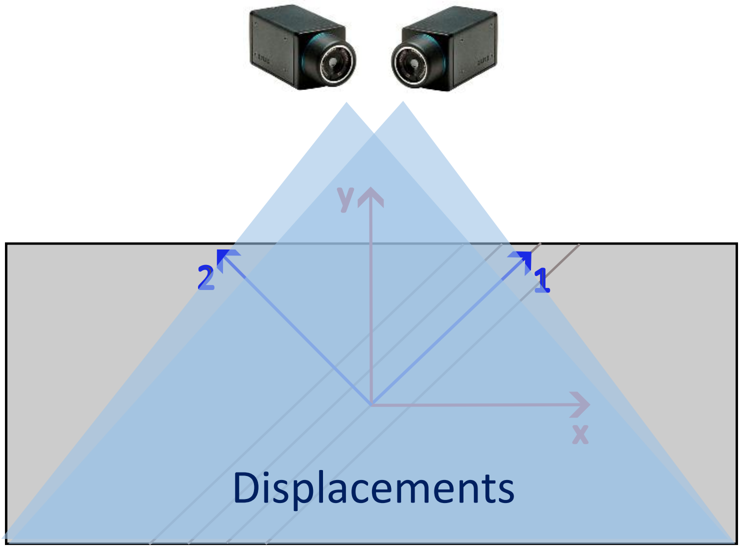

1,2: Ply coordinate system

x,y: Laminate coordinate system

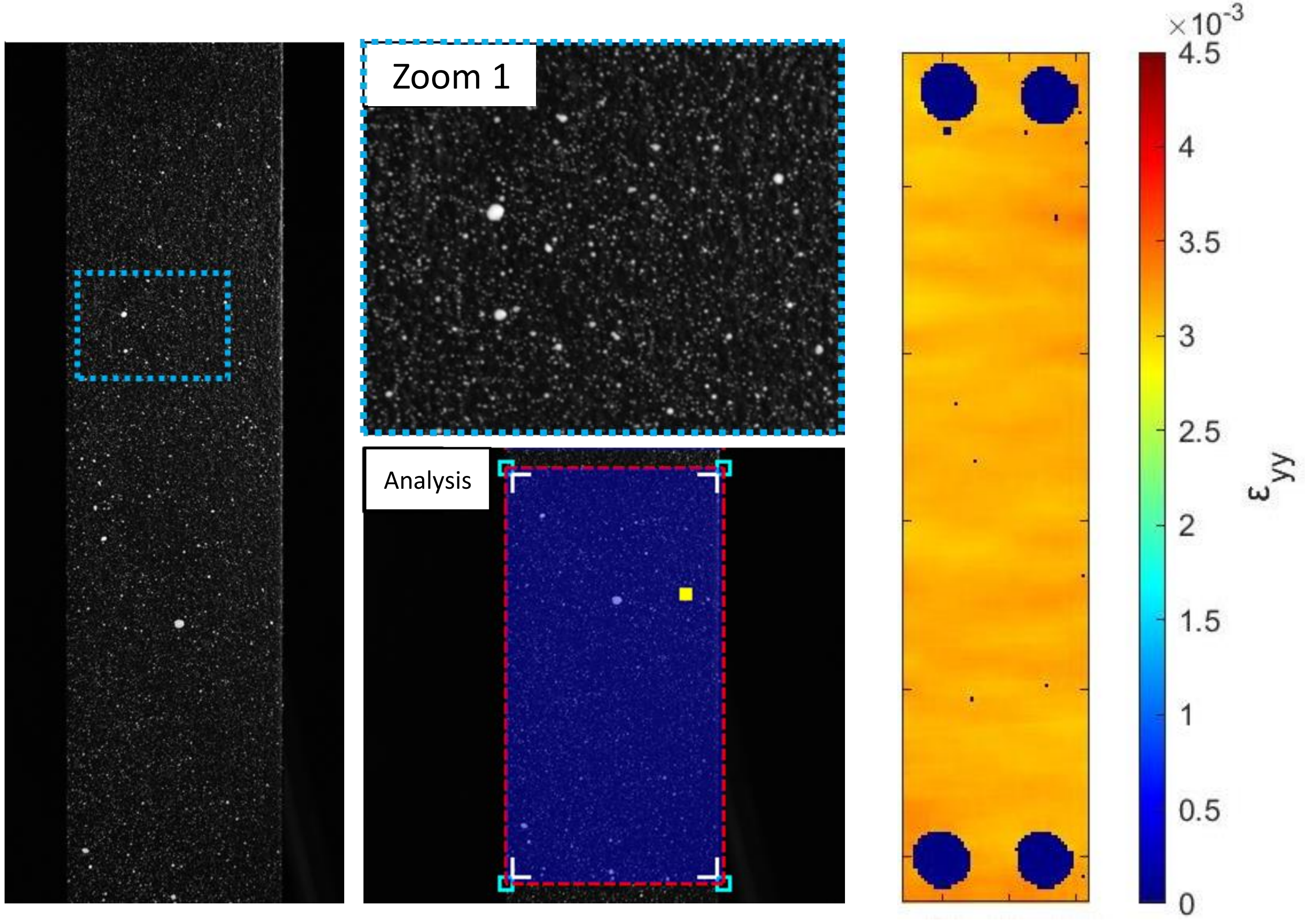

ε_{xx} CHANGE WITH LOADING FREQUENCY

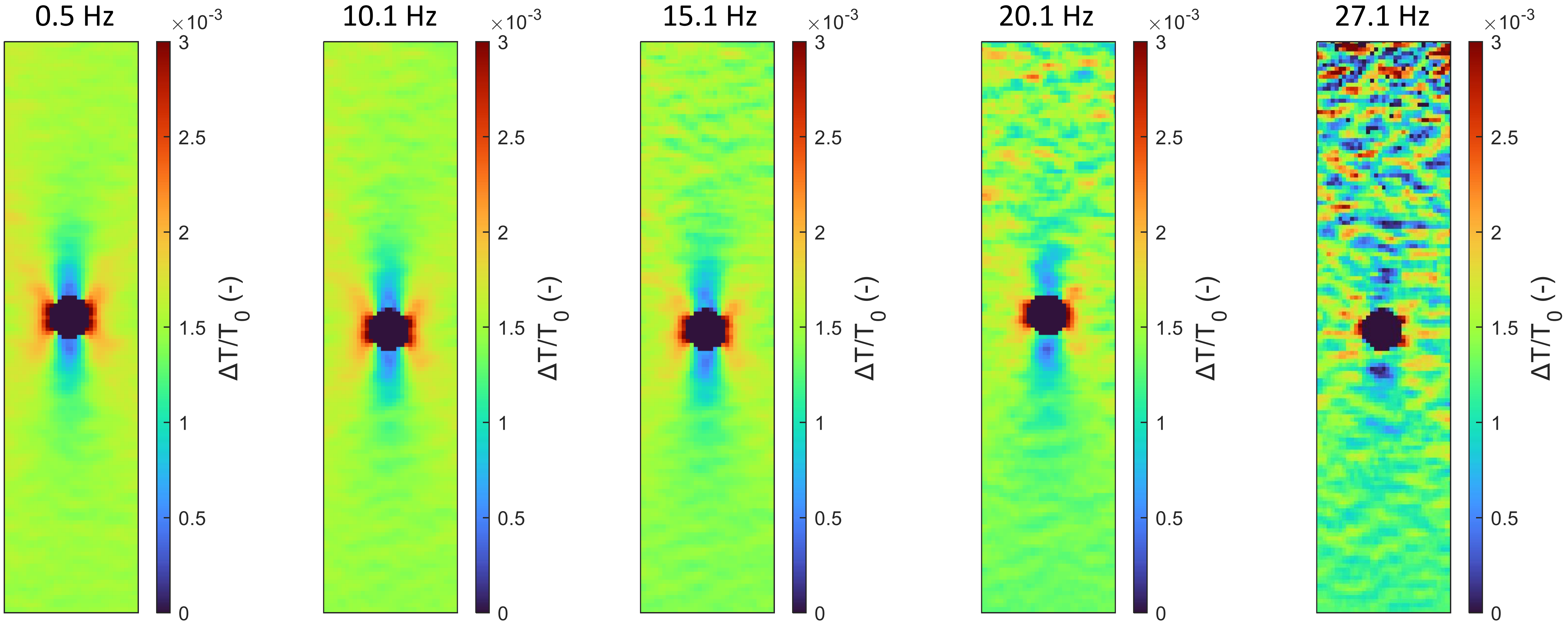

THERMAL CAMERAS / Comparison

Model	Telops FAST IR MK2	FLIR AC655	FLIR Lepton 3.5
Type	Photon Detector	Micro-bolometer	PCB mounted micro-bolometer
Sensor size	256 x 320 pixels	480 x 640 pixels	120 x 160 pixels
Sensitivity	25 mk	50 mK	50 mK
Size	321 × 199 × 176 mm	216 × 73 × 75 mm	10 × 12 × 7 mm
Cost	~ 100k GBP	~10k GBP	~300 GBP

THERMAL CAMERAS / Comparison

Photondetectors datasheet [1]

Characteristics	Photon Detector	
IR Camera	FLIR SC5500	Telops FAST M2k
Detector material	InSb	
Spectral range	2.5 - 5.1 µm	1.5 - 5.4 µm
Pixel dimension	30 µm	25 µm
Cost	~£100,000	
Maximum frame rate at full window	383 Hz	1910 Hz
Frame rate selection	Any value up to 383 Hz	Any value up to 1910 Hz
Reading array	All pixel detectors at the same time	
Integration time	10 - 20,000 µs	0.27 µs to 513 µs
Response time	10 - 20,000 µs	0.27 µs to 513 µs
Sensitivity (NETD)	<20 mK	<25 mK
Resolution	320 x 256 pixels	
Cooling	Yes	
Analogue input	Yes	
Weight	3.8 kg	< 6 kg
Size	310 x 141 x 159 mm	321 x 199 x 176 mm

Microbolometers datasheet [1]

Characteristics	Standard microbolometer	Thermal core microbolometer
IR Camera	FLIR A655sc	FLIR Lepton 3.5 radiometric
Detector material	VOx	VOx
Spectral range	7.5 - 14 µm	8 - 14 µm
Pixel dimension	17 µm	12 µm
Cost	~£10,000	~£500
Maximum frame rate at full window	50 Hz	Limited at 8.7751 Hz
Frame rate selection	50 Hz, 25 Hz, 12.5 Hz, 6.25 Hz, 3.13 Hz	8.7751 Hz
Reading array	Each row of pixels at a time	
Thermal time constant	8 ms - fixed	12 ms
Response time	24 ms (3 x thermal time constant)	36 ms (3 x thermal time constant)
Sensitivity (NETD)	< 30 mK	< 50 mK
Resolution	640 x 480 pixels	160 x 120 pixels
Cooling	No	
Analogue input	No	
Weight	0.9 kg	0.9 g
Size	216 x 73 x 75 mm	10.50 x 12.70 x 7.14 mm

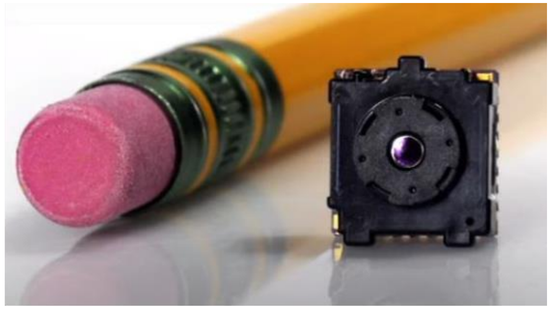

FLIR Lepton 3.5 radiometric

[1] Irene Jiménez-Fortunato. Development and integration of full-field imaging techniques for assessment of composite structures. 2021.

TSA VIDEOS

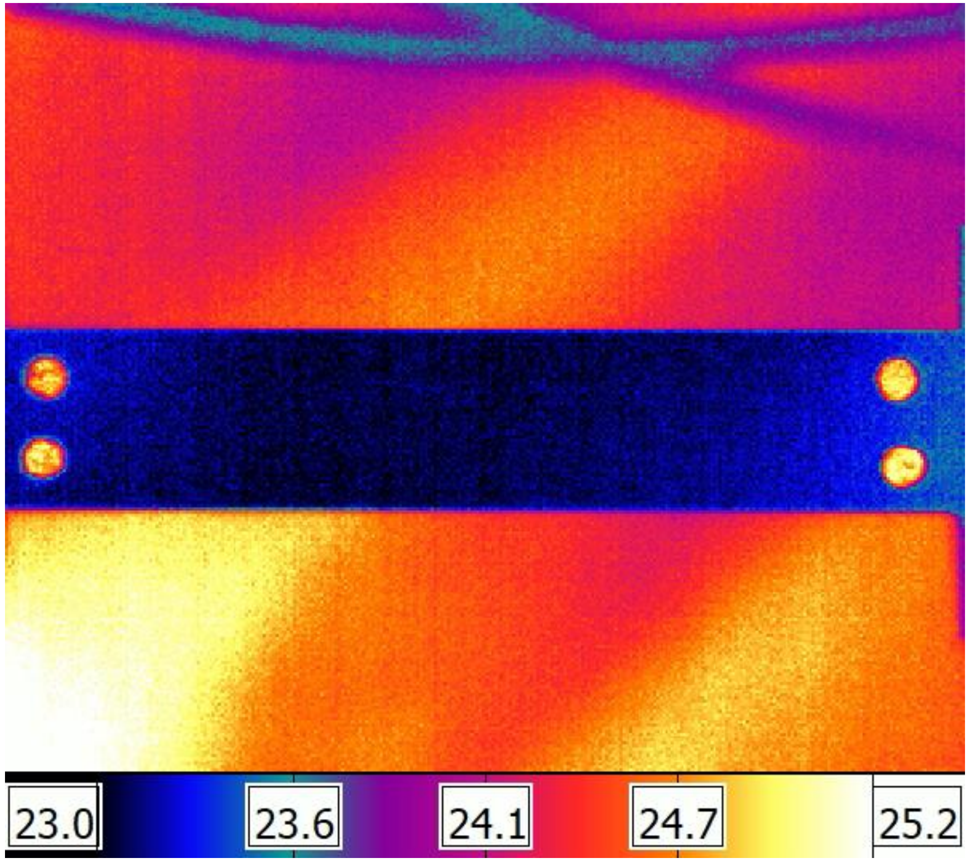

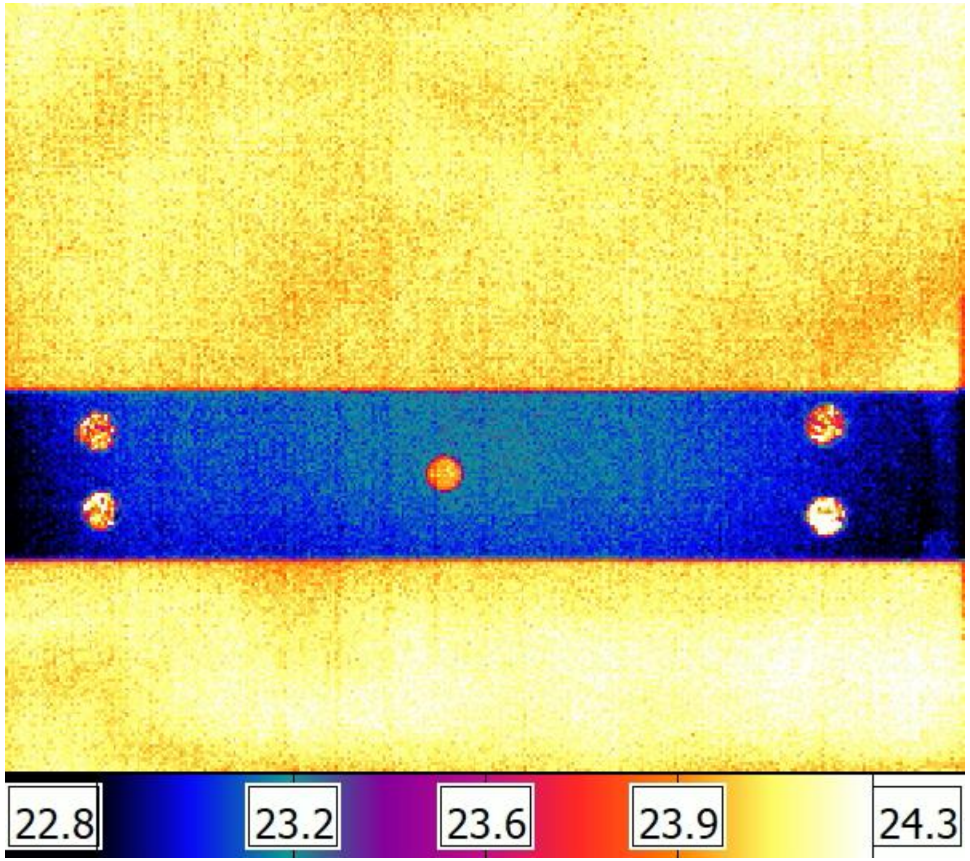

Lock-in filtering approach

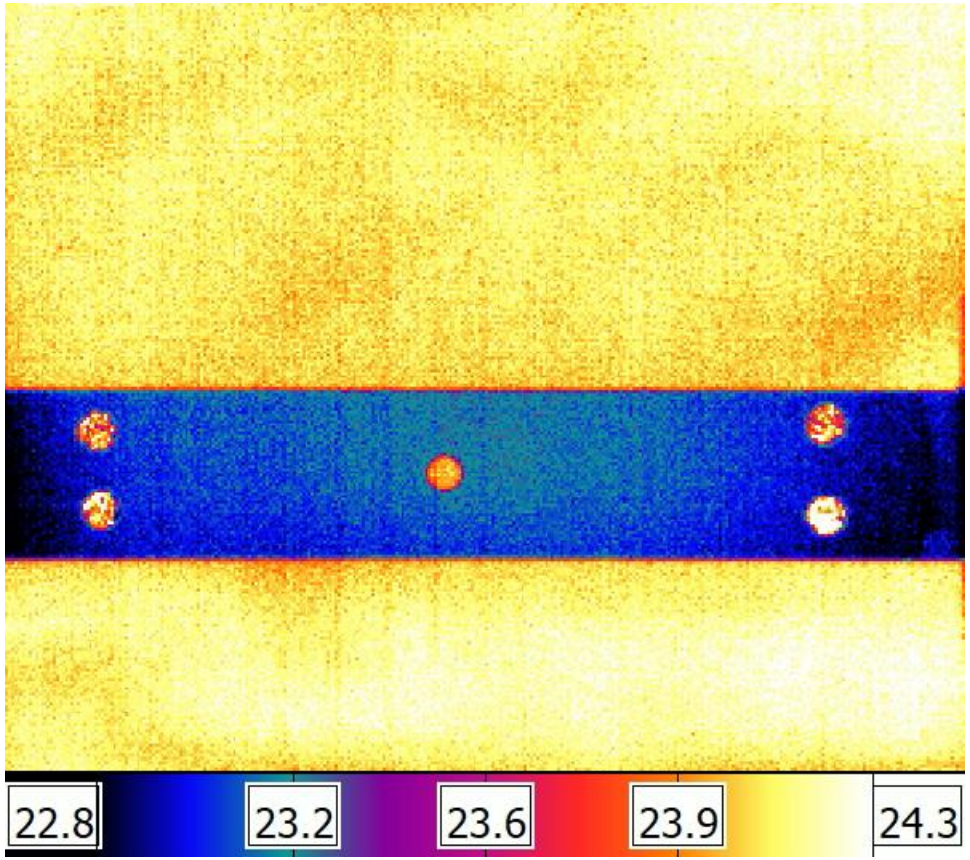

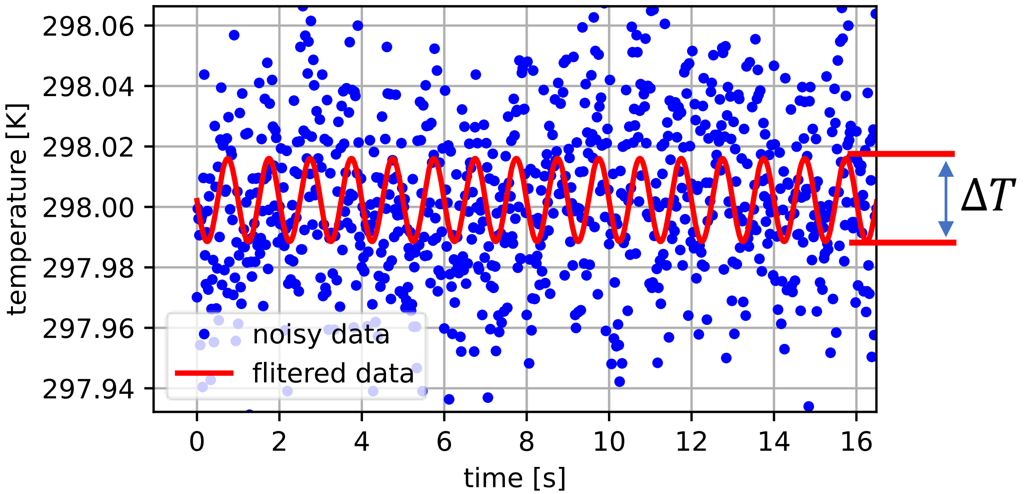

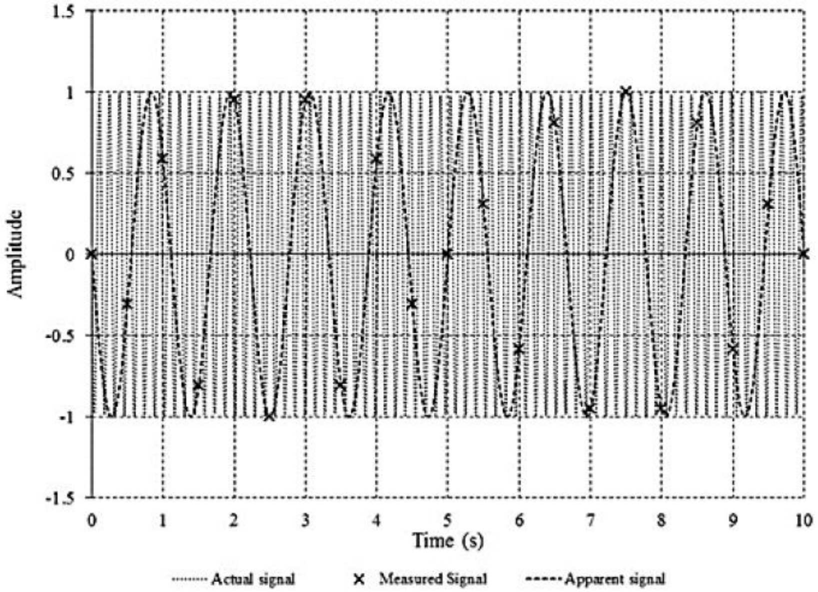

The resin influence on Strip specimens TSA Results

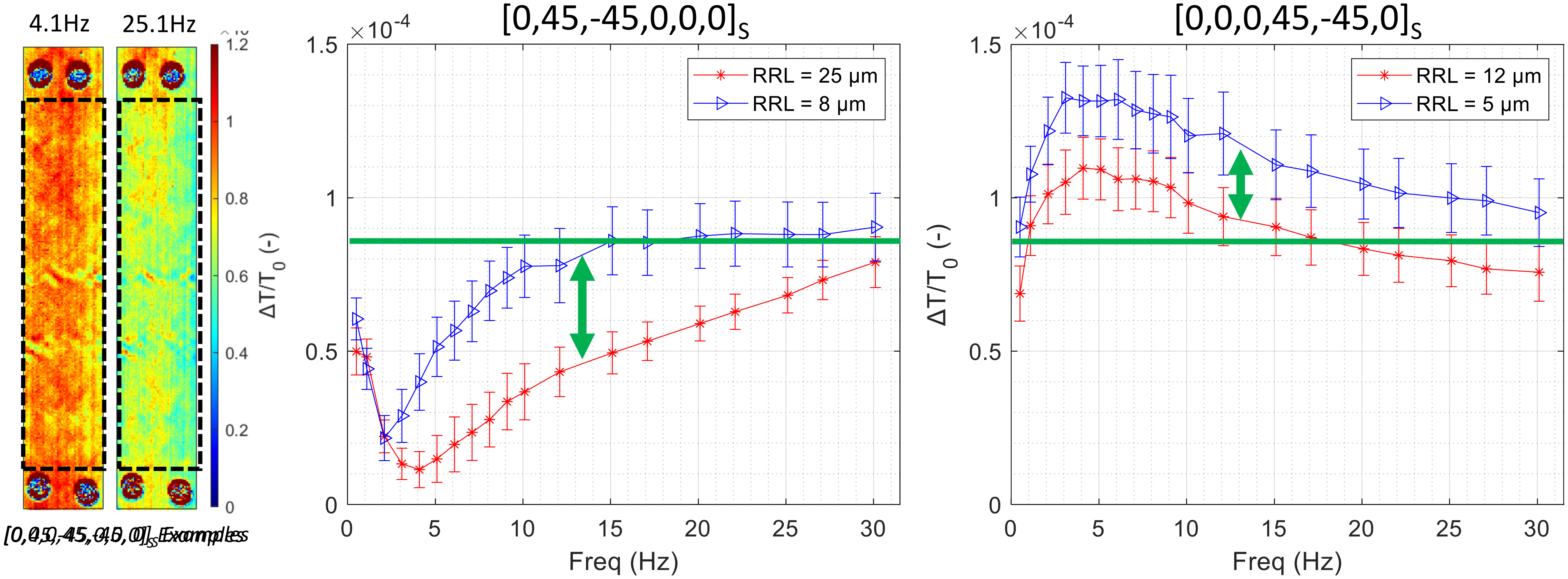

The trend of ***ΔT/T*₀ is different for the two configurations** with loading frequency.

Both layups **"converge" to a similar level** at high frequencies.

The **RRL** has an influence on *ΔT* and **changes the response** in this frequency domain (0.5 – 30.1 Hz).

$[0,45,-45,0,0,0]_S$

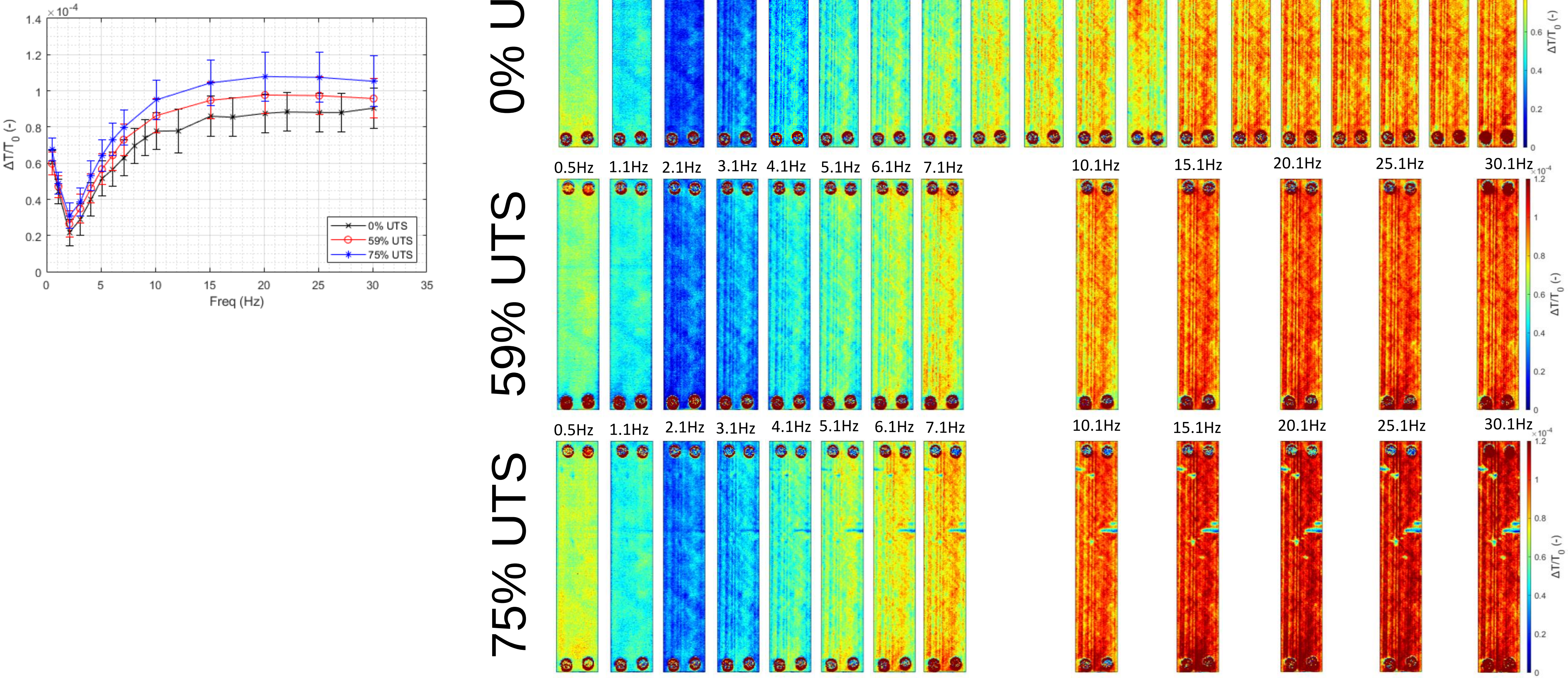

ΔT/T0 (-)
Freq (Hz)
0% UTS
59% UTS
75% UTS
0.5Hz
1.1Hz
2.1Hz
3.1Hz
4.1Hz
5.1Hz
6.1Hz
7.1Hz
8.1Hz
9.1Hz
10.1Hz
12.1Hz
15.1Hz
17.1Hz
20.1Hz
22.1Hz
25.1Hz
27.1Hz
30.1Hz

$[0,0,0,45,-45,0]_s$

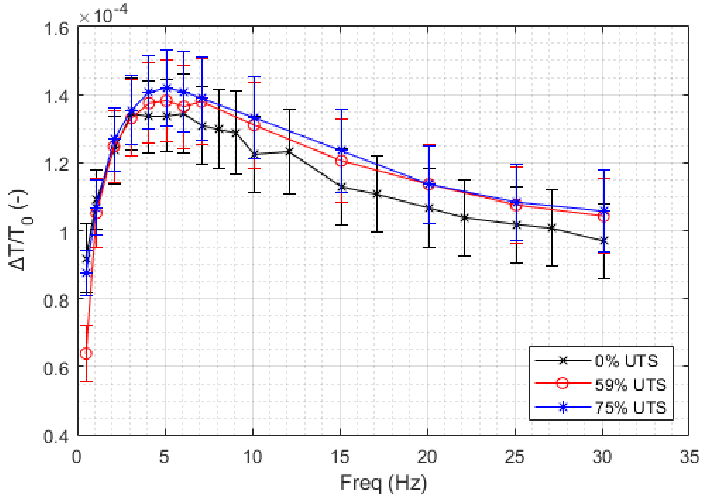

×10⁻⁴
1.6
1.4
1.2
1
0.8
0.6
0.4
ΔT/T₀ (-)
0
5
10
15
20
25
30
35
Freq (Hz)
0% UTS
59% UTS
75% UTS

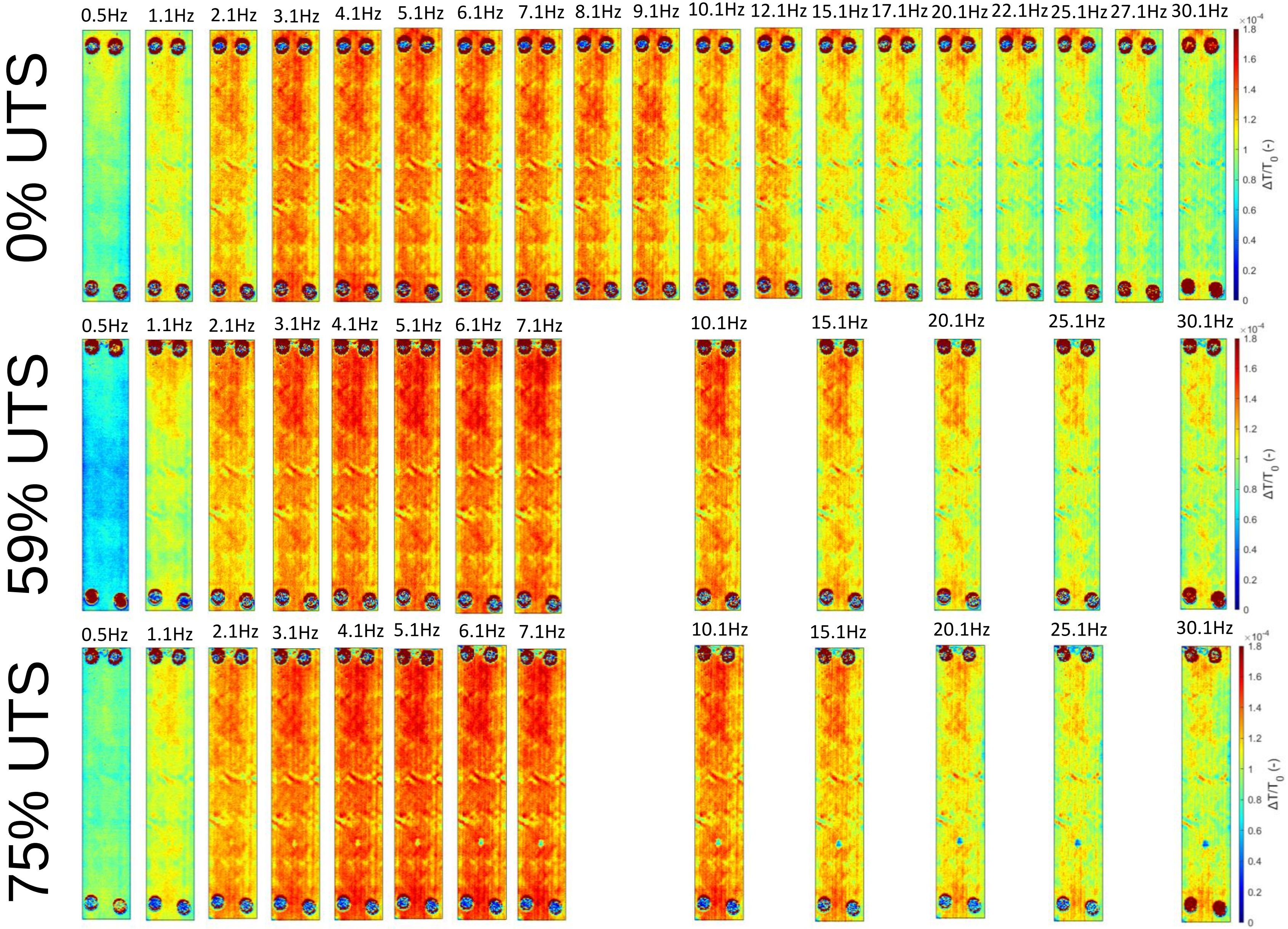

0% UTS
0.5Hz 1.1Hz 2.1Hz 3.1Hz 4.1Hz 5.1Hz 6.1Hz 7.1Hz 8.1Hz 9.1Hz 10.1Hz 12.1Hz 15.1Hz 17.1Hz 20.1Hz 22.1Hz 25.1Hz 27.1Hz 30.1Hz
59% UTS
0.5Hz 1.1Hz 2.1Hz 3.1Hz 4.1Hz 5.1Hz 6.1Hz 7.1Hz 10.1Hz 15.1Hz 20.1Hz 25.1Hz 30.1Hz
75% UTS
0.5Hz 1.1Hz 2.1Hz 3.1Hz 4.1Hz 5.1Hz 6.1Hz 7.1Hz 10.1Hz 15.1Hz 20.1Hz 25.1Hz 30.1Hz
ΔT/T₀ (-)

TSA Results / OH $[0,45,-45,0,0,0]_S$

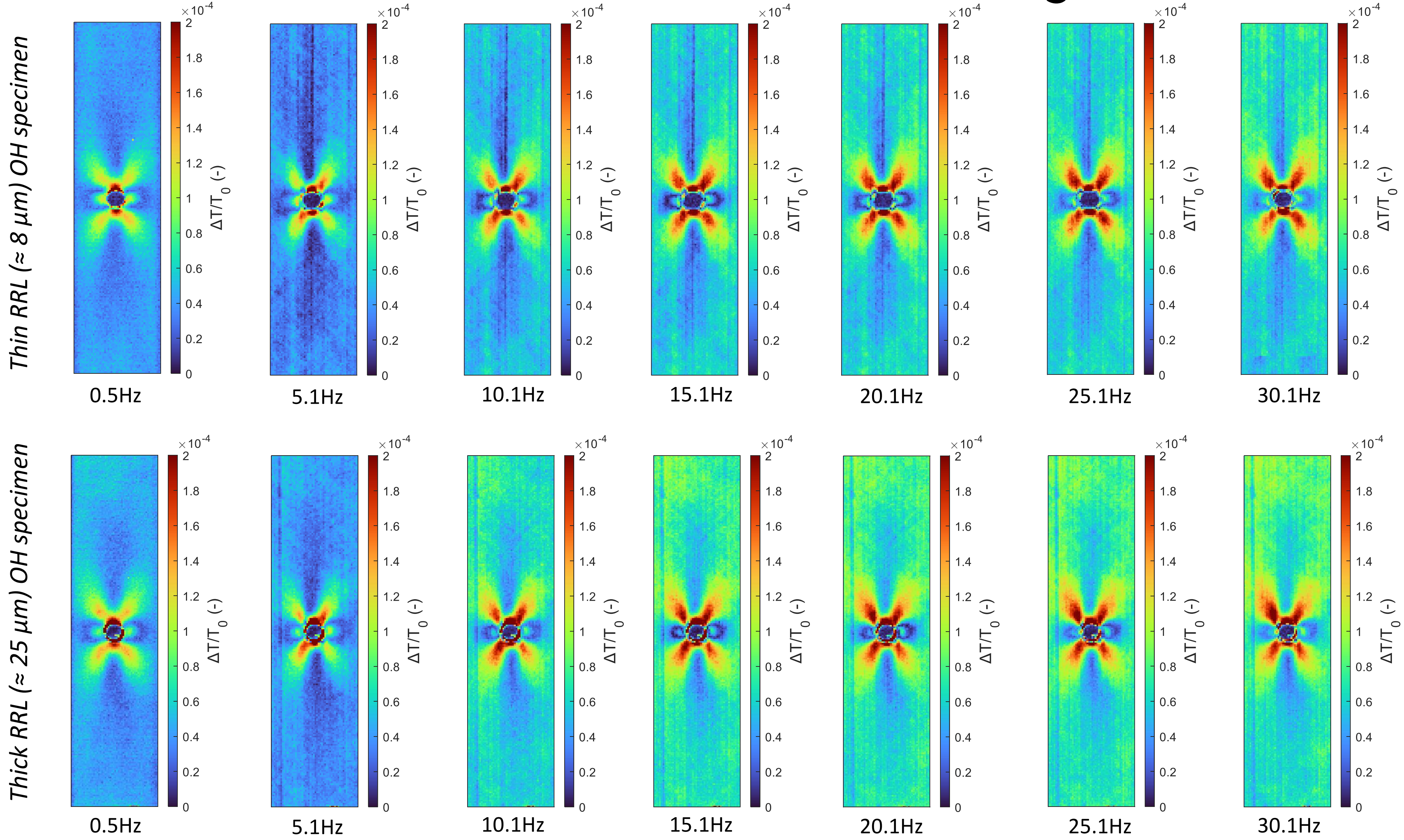

TSA Results / OH $[0,0,0,45,-45,0]_S$

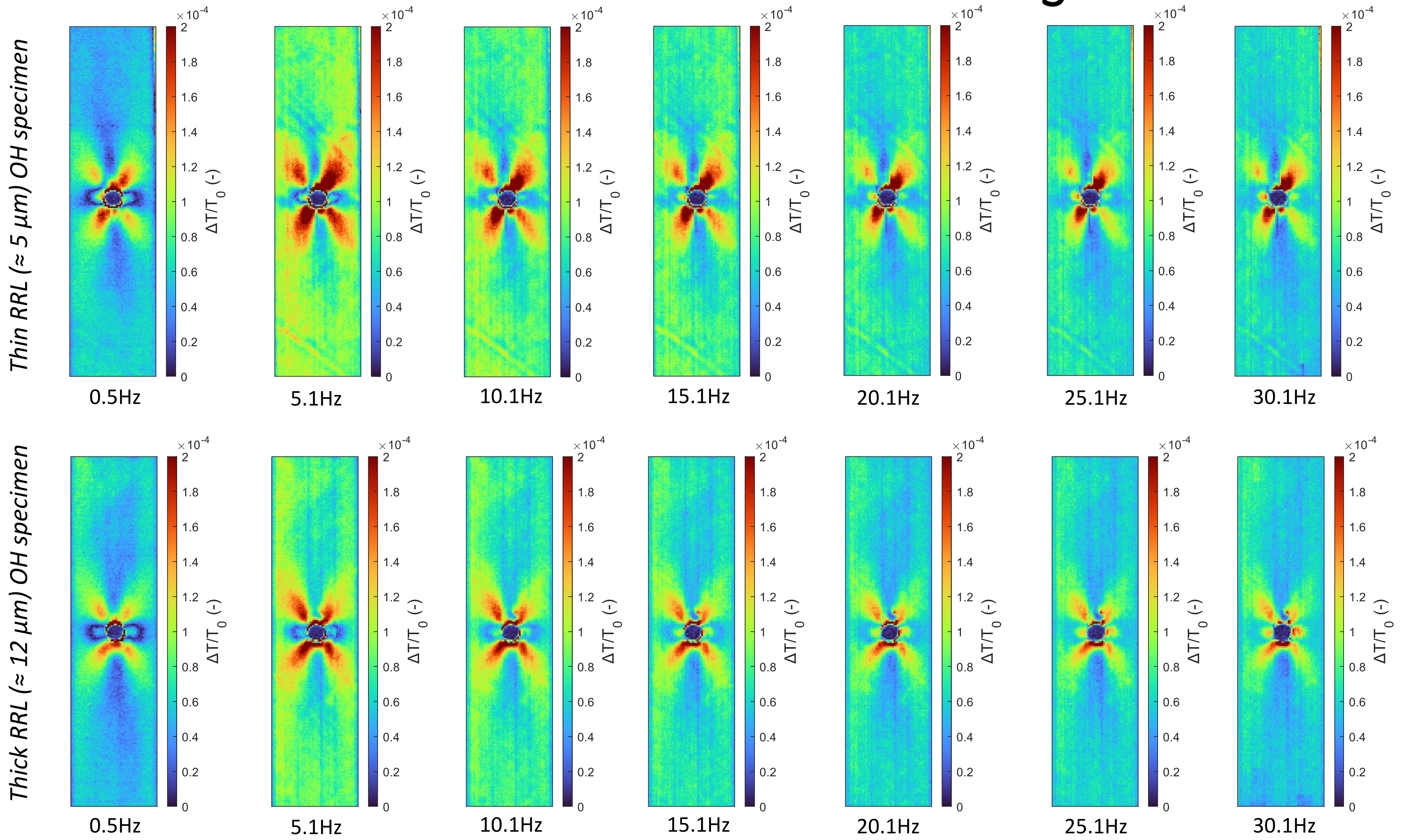

TSA PHASE FULL FIELD IMAGES

$[0,45,-45,0,0,0]_S$

$[0,0,0,45,-45,0]_S$

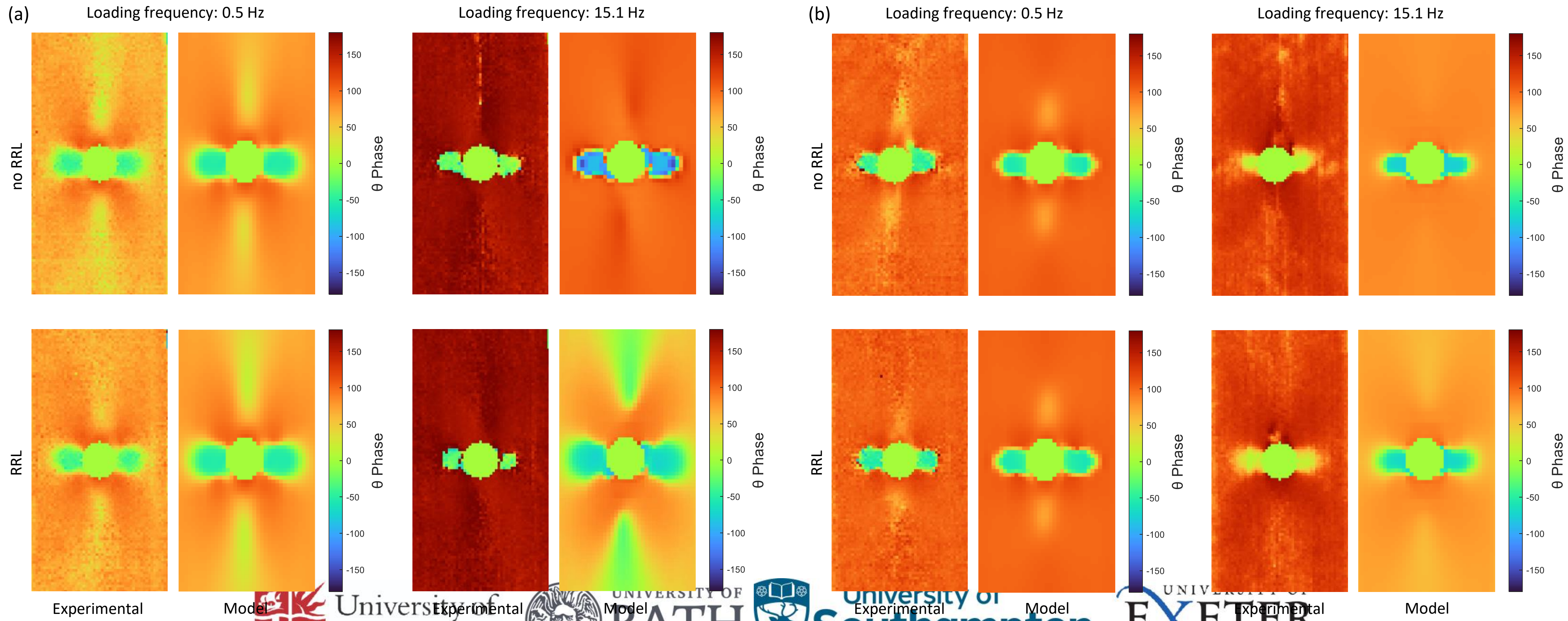

TSA EXPERIMENTAL MODELS

Resin Rich Layer Model $\Delta\varepsilon_{DIC} \rightarrow \Delta T_{RRL}$

$$\frac{\Delta T_r}{T_0} = -\frac{e\alpha_r}{\rho_r C_{p_r}}\left[\frac{E_r}{1-\nu_r}\left(\Delta\varepsilon_x + \Delta\varepsilon_y\right) + G_r \Delta\varepsilon_{xy}\right]$$

Global Laminate Model $\Delta\varepsilon_{DIC} \rightarrow \Delta T_{Laminate}$

$$\frac{\Delta T_{laminate}}{T_0} = -\frac{e}{\rho C_p}\begin{bmatrix}\alpha_x & \alpha_y & \alpha_{xy}\end{bmatrix}[A^*]\begin{bmatrix}\Delta\varepsilon_x \\ \Delta\varepsilon_y \\ \Delta\varepsilon_{xy}\end{bmatrix}$$

Surface Ply Model $\Delta\varepsilon_{DIC} \rightarrow \Delta T_{S.Ply}$

$$\frac{\Delta T_{surfaceply}}{T_0} = -\frac{e}{\rho C_p}\begin{bmatrix}\alpha_1 & \alpha_2 & 0\end{bmatrix}\begin{bmatrix}\frac{E_1}{1-\nu_{12}\nu_{21}} & \frac{\nu_{21}E_1}{1-\nu_{12}\nu_{21}} & 0 \\ \frac{\nu_{21}E_1}{1-\nu_{12}\nu_{21}} & \frac{E_2}{1-\nu_{12}\nu_{21}} & 0 \\ 0 & 0 & G_{12}\end{bmatrix}[T_e]\begin{bmatrix}\Delta\varepsilon_x \\ \Delta\varepsilon_y \\ \Delta\varepsilon_{xy}\end{bmatrix}$$

Jiménez-Fortunato, D.J. Bull, O.T. Thomsen, J.M. Dulieu-Barton, Composites Part A: Applied Science and Manufacturing 149 (2021)

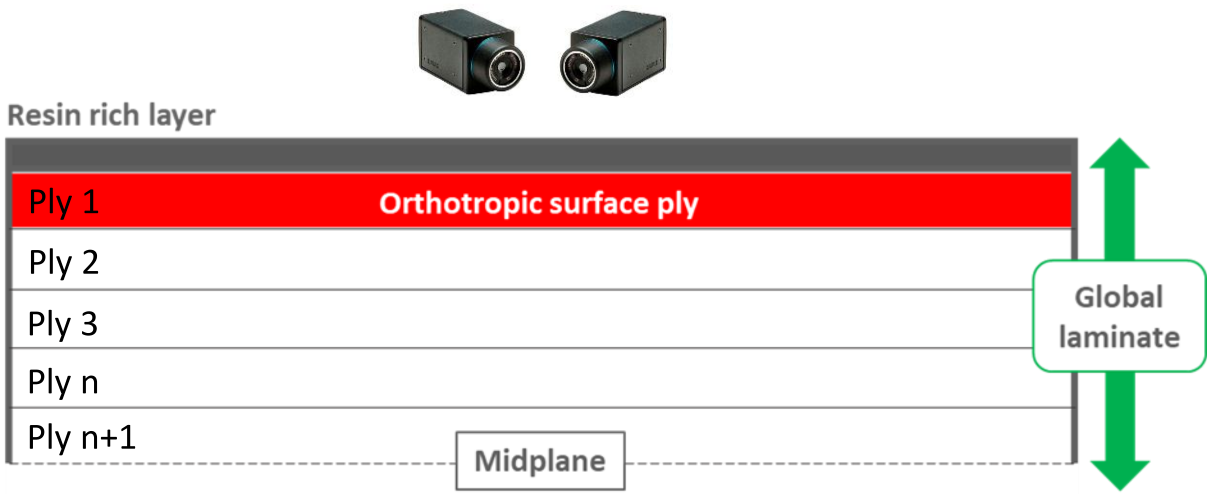

FEA NUMERICAL MODEL

Via a Python script, a parametric model has been developed in Abaqus:

- **Geometry (H, W)** of the specimen, **number (N)** and **thickness (T)** of plies, **lay-up**, **material system** are fully customisable.
- Inclusion of a superficial **resin-rich layer (RRL).**
- Symmetric **displacement** with a **sinusoidal waveform** applied to upper and lower faces of the specimen.
- **Conduction** between plies.
- **Coupled temperature-displacement analysis** (C3D8T brick elements).

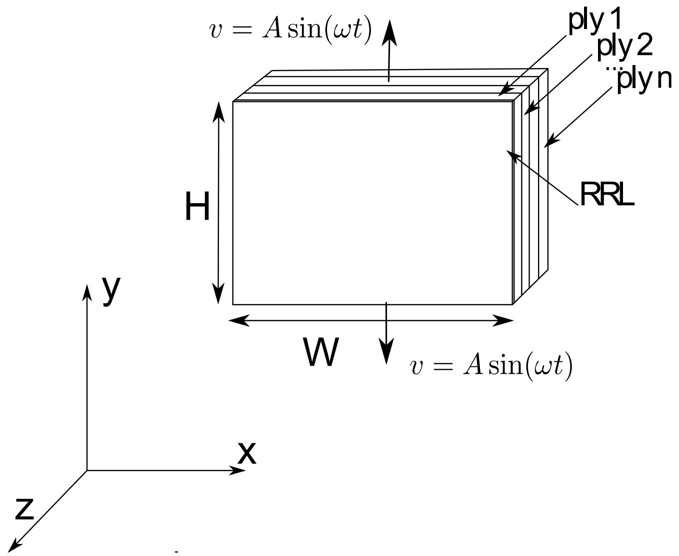

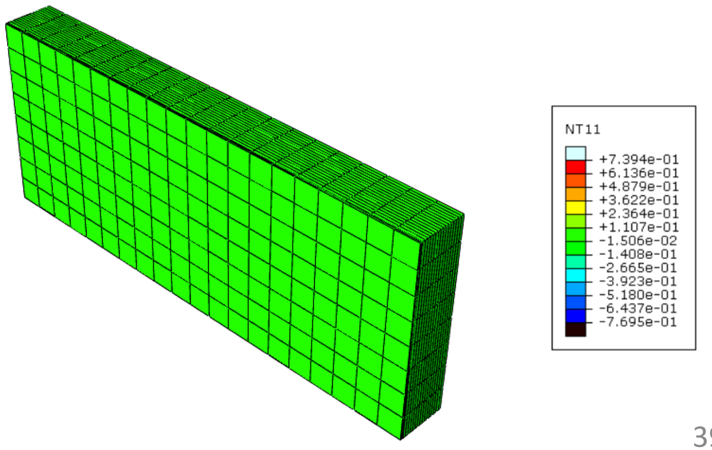

*For more details on the model: Cappello, Riccardo, Giuseppe Pitarresi, and Giuseppe Catalanotti. "Thermoelastic Stress Analysis for composite laminates: A numerical investigation." *Composites Science and Technology* (2023): 110103.

TSA & FEA Model Results - Around the hole

OH $[0,45,-45,0,0,0]_S$

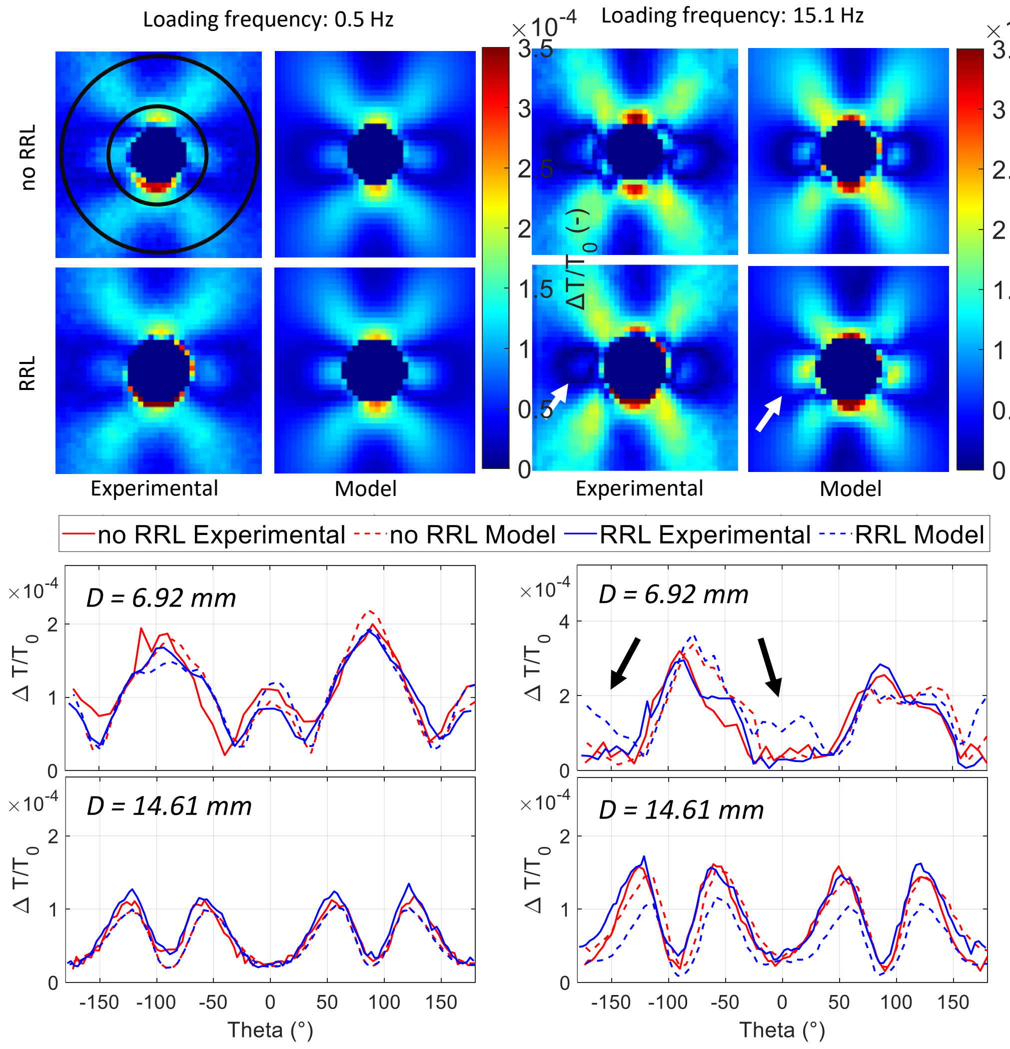

OH $[0,0,0,45,-45,0]_S$

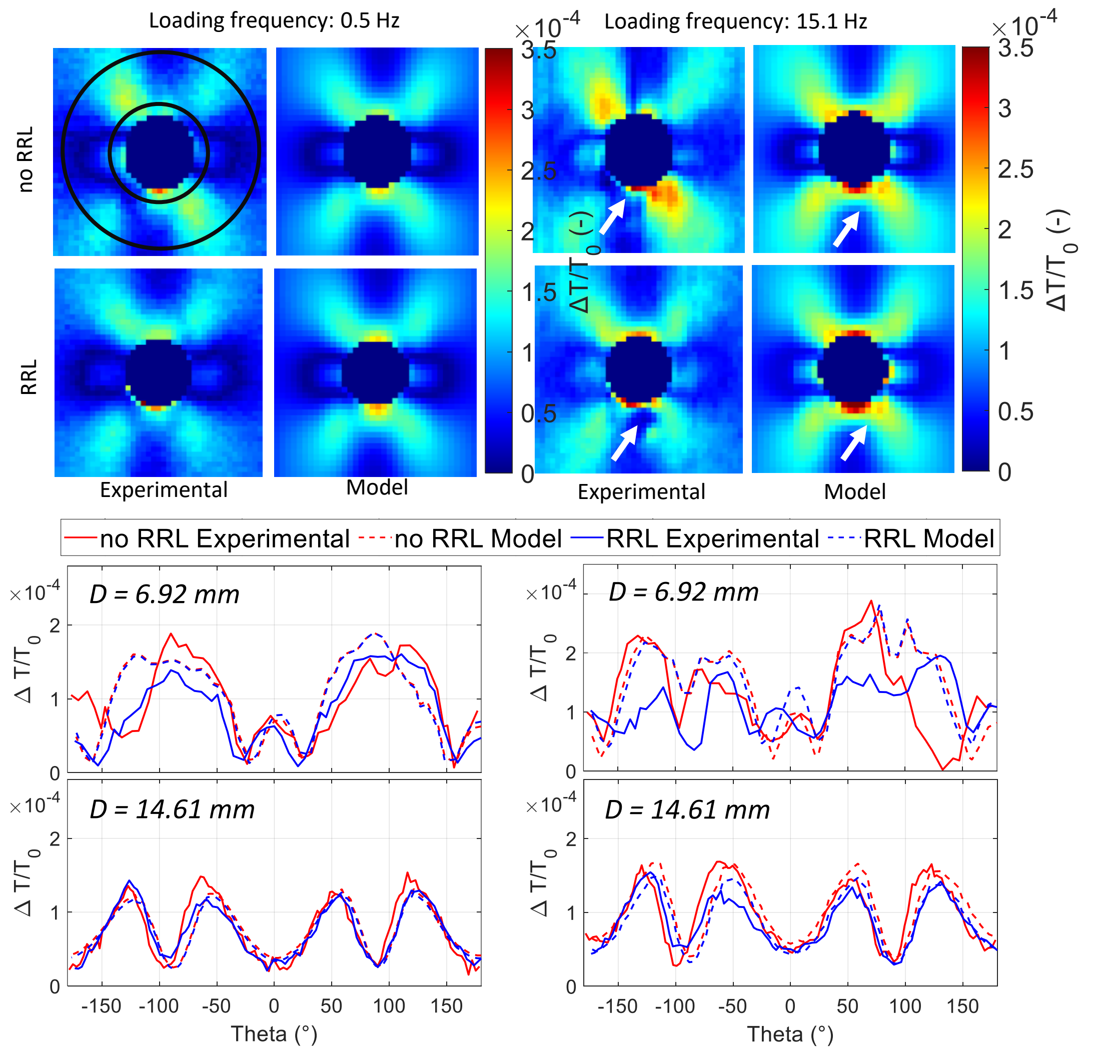

TSA & FEA Model Results - Around the hole

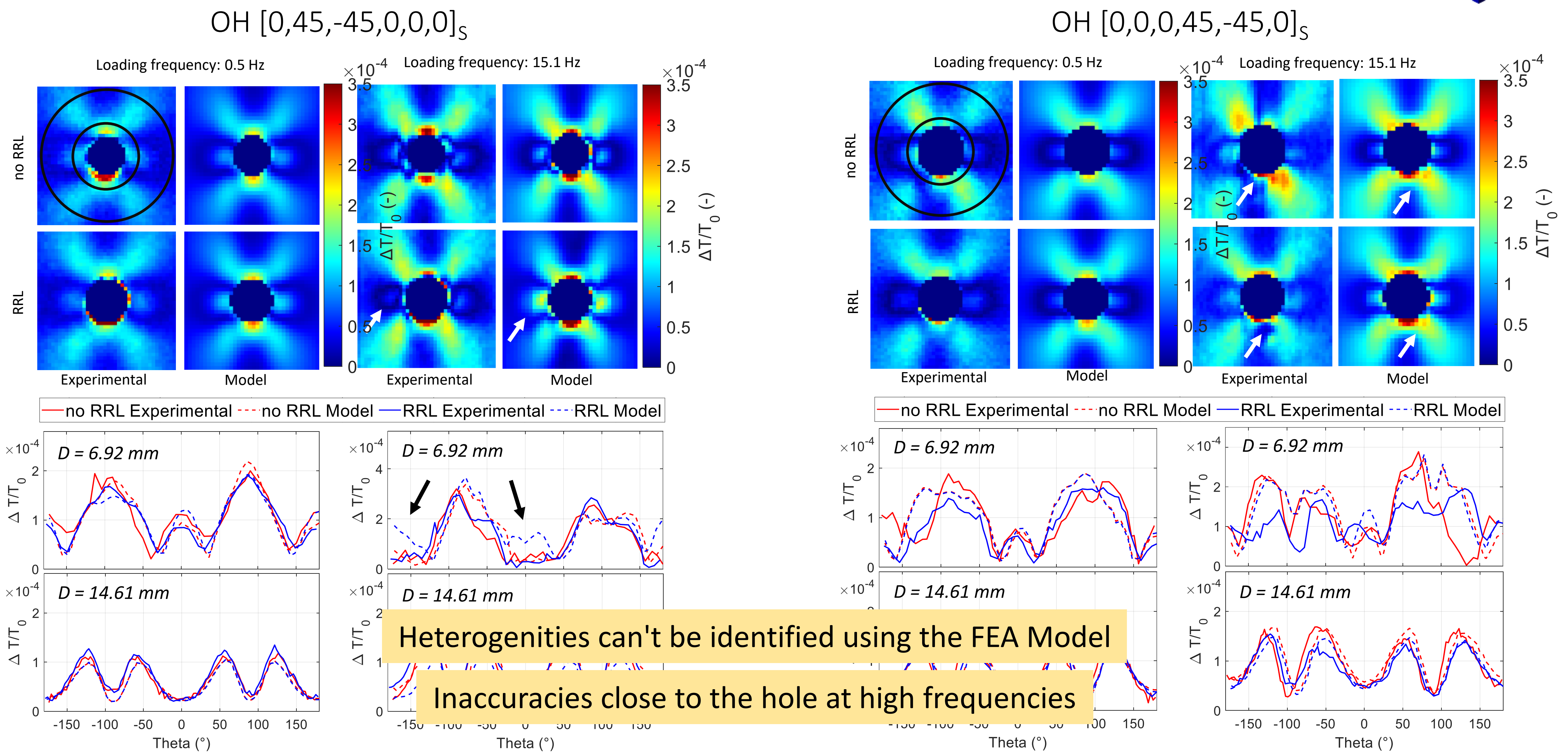

Heterogenities can't be identified using the FEA Model

Inaccuracies close to the hole at high frequencies

Through thickness TSA analysis – FEA Model

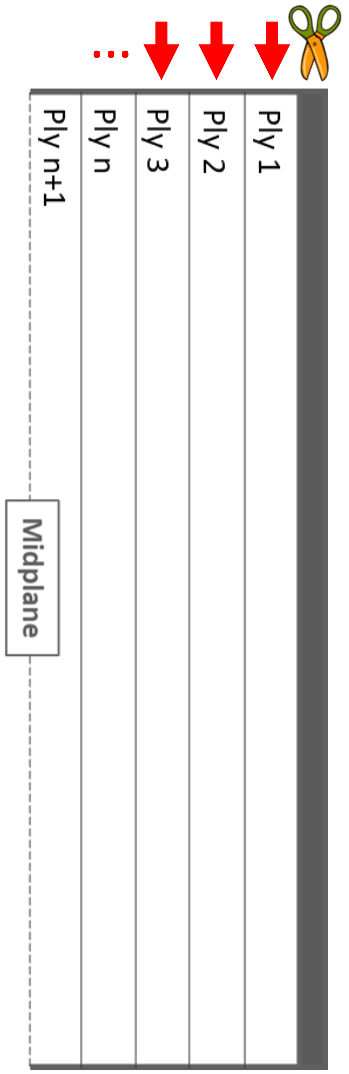

Loading Frequency: 15.1 Hz

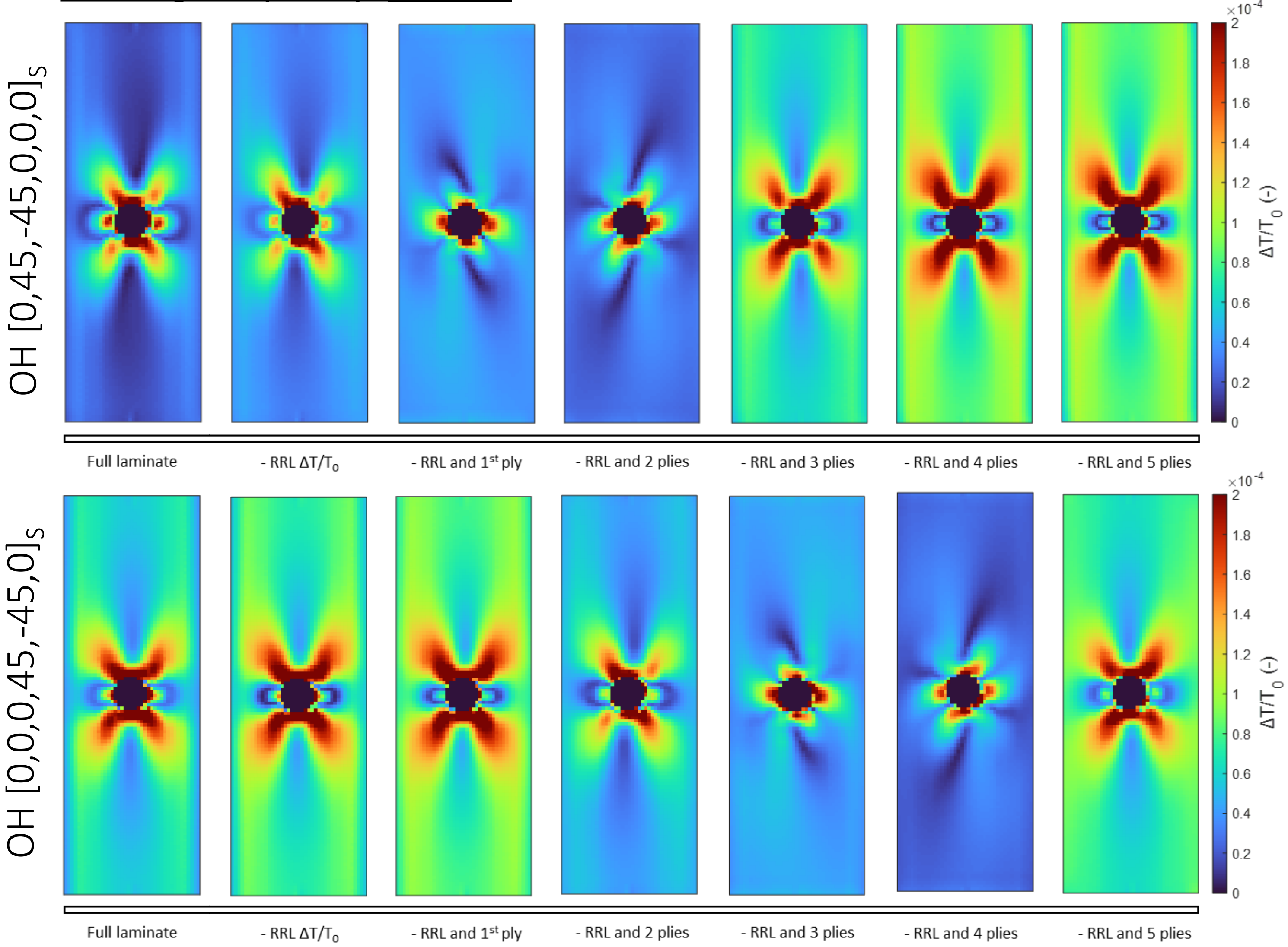

↓Heat transfer between the plies

Different stress state for each ply

Different **temperature fields**

Tending to adiabaticity.
Still heat transfer between the plies

Measuring the $K_{t.thickness}$ (The Flash Method)

Main literature reference: 0.84 W/m*K [5]

[5] M.T. Saad, S.G. Miller, T. Marunda, Thermal characterization of IM7/8552-1 carbon-epoxy composites, ASME 2014 Int. Mech. Eng. Congr. Expos. (2014) 1–8.

Table 1. Thermal Properties of IM7/8552-1 Composite

Temperature (°C)	Thermal Diffusivity (cm^2/s)	Specific Heat (J/g*K)	Thermal Conductivity (W/m*K)
25	0.0068	0.85741	0.84126
50	0.0067	0.91981	0.88184
75	0.0065	0.98683	0.92572
100	0.0064	1.05835	0.97286
125	0.0063	1.13099	1.02034
150	0.0062	1.20378	1.06764
175	0.0061	1.28975	1.12186

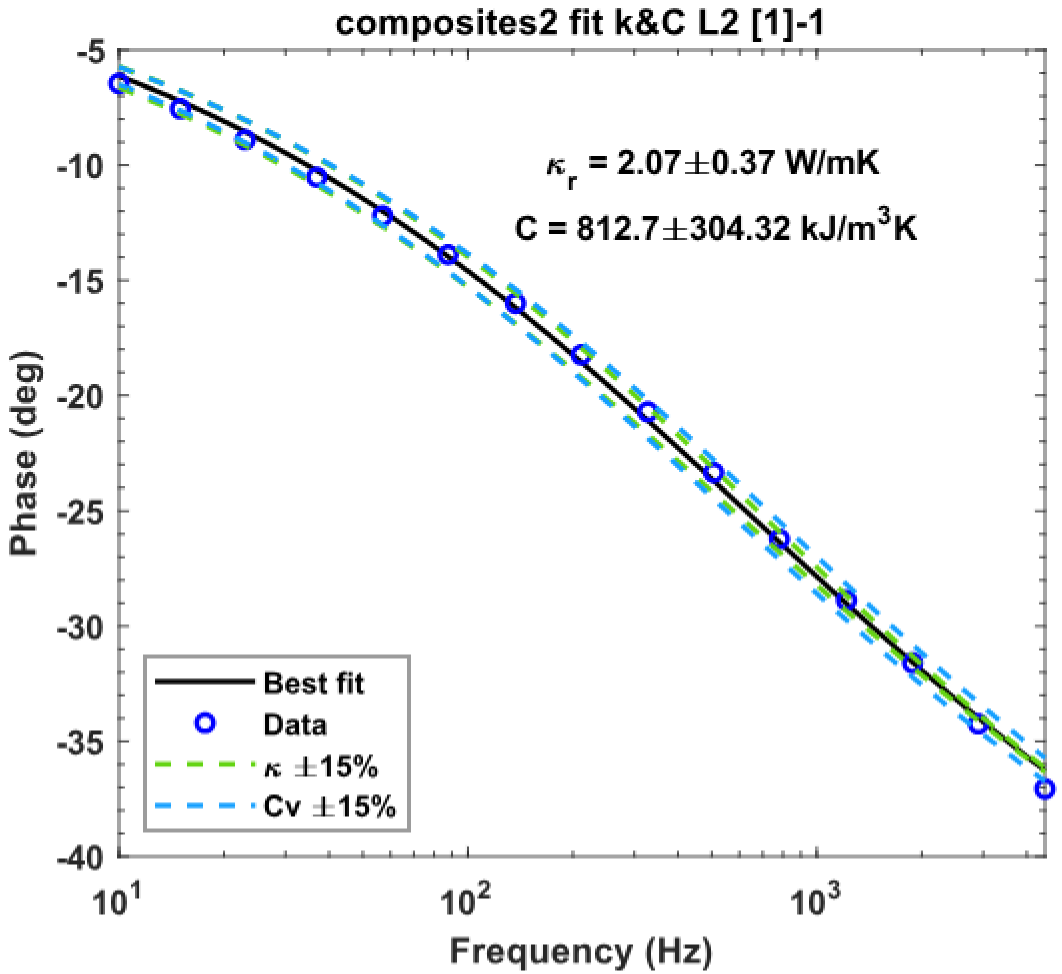

The flash method

- The power source can be a laser or a flash lamp.
- The energy will then be absorbed by the specimen and emitted again on the top of the sample.
- This radiation results in a temperature rise on the surface of the sample.
- This temperature rise is recorded from an infrared (IR) detector.

The Flash Method

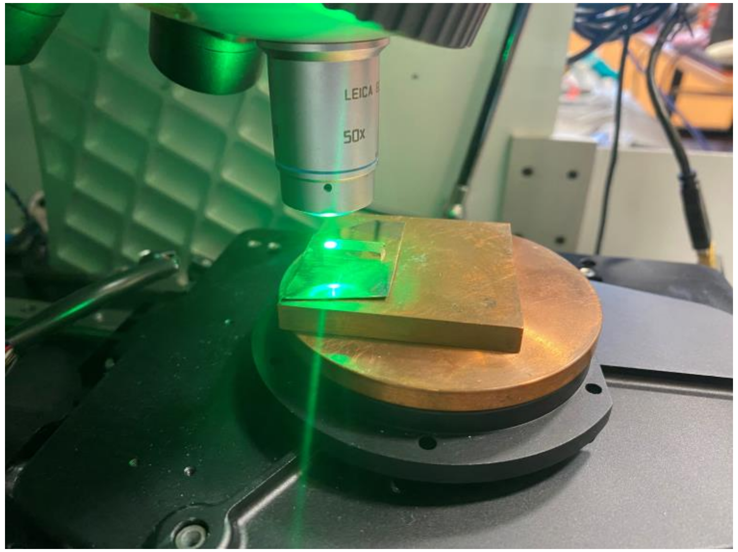

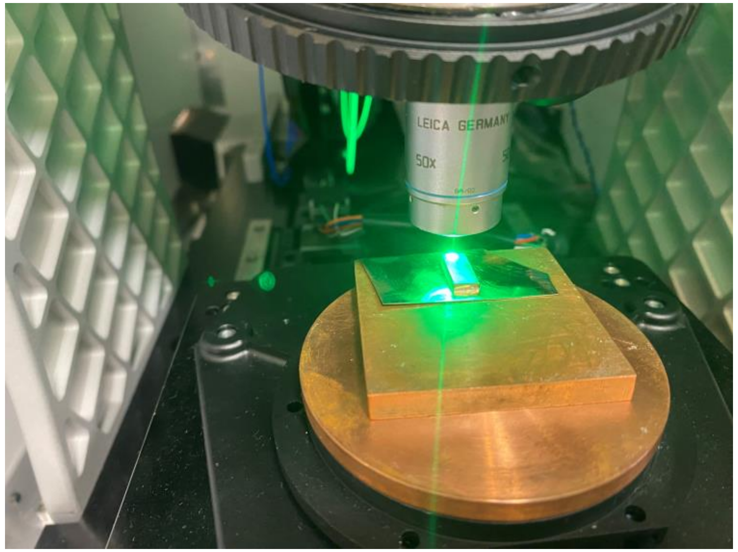

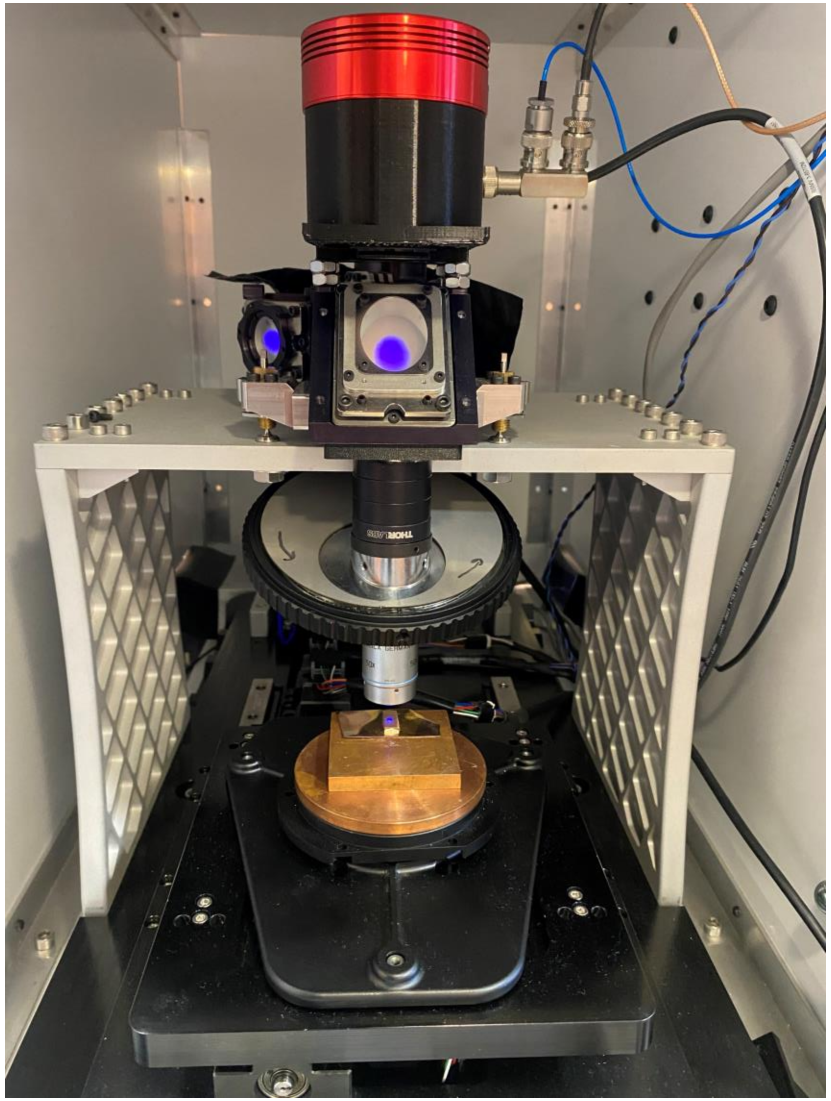

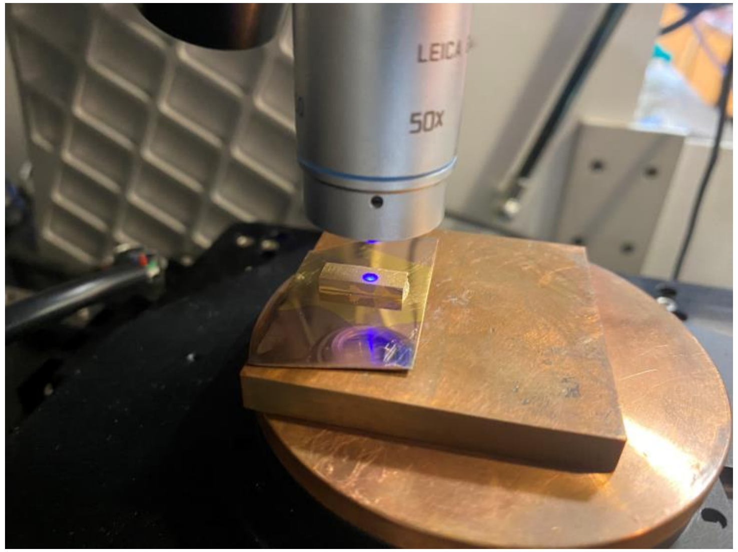

NUMERICAL MODEL WITH DIFFERENT $K_{t.thickness}$

Low K (0.6 W/m*K)

OH $[0,45,-45,0,0,0]_S$

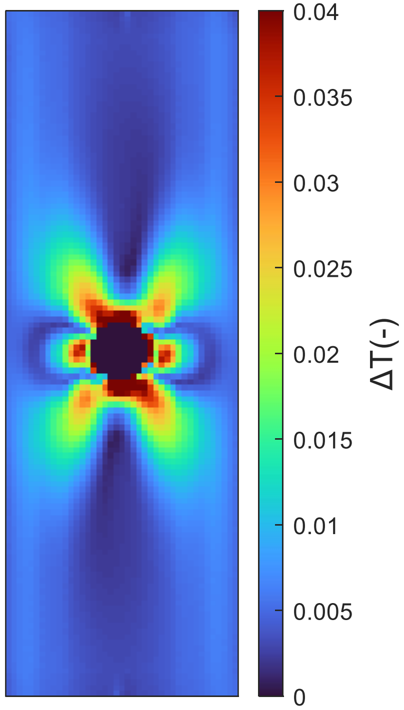

OH $[0,0,0,45,-45,0]_S$

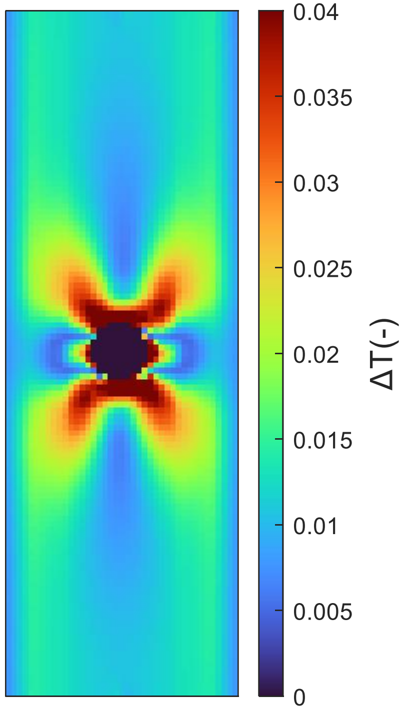

High K (2.07 W/m*K)

OH $[0,45,-45,0,0,0]_S$

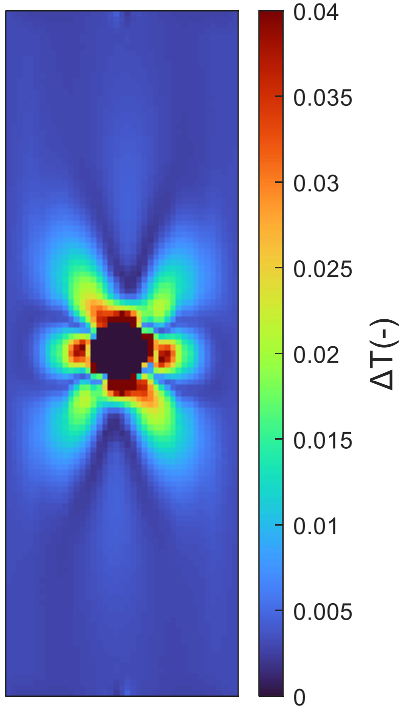

OH $[0,0,0,45,-45,0]_S$

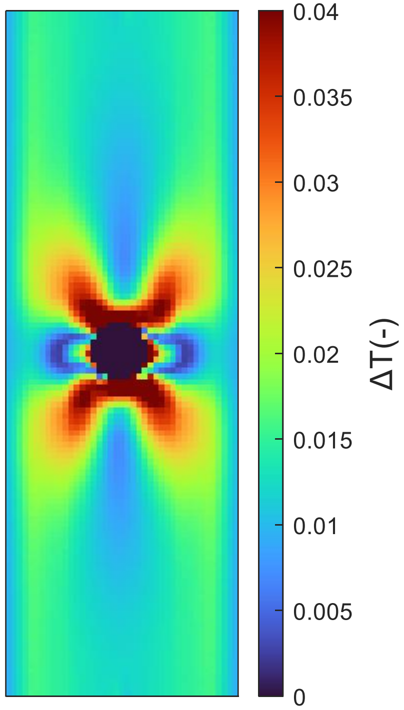

**Loading frequency: 15.1Hz*

FULL FIELD Ply by Ply $\Delta T/T_0$ - TSA Models (Residuals)

Exp. FEA

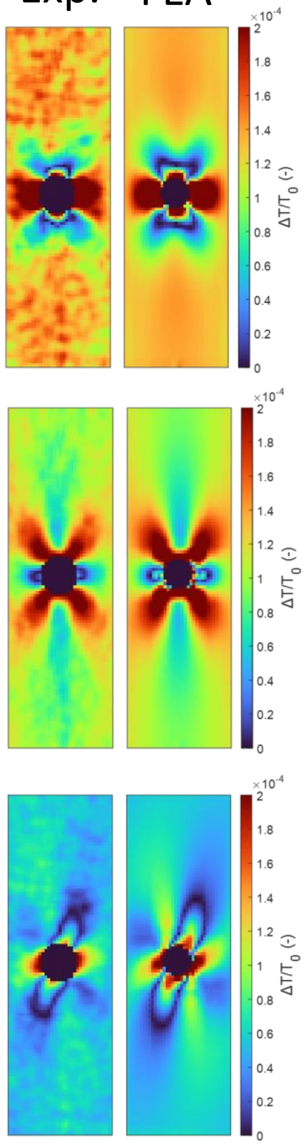

Subtraction

FEA Model – Experimental models

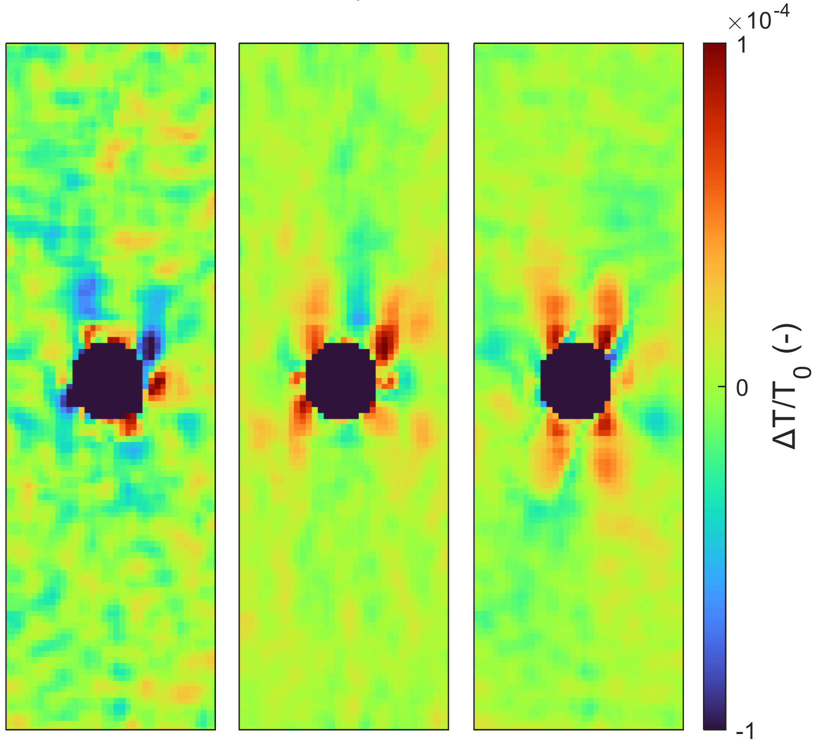

Resin M. 0° Ply M. 45° Ply M.

FULL FIELD STRAIN ANALYSIS AND FEDEF (Residuals)

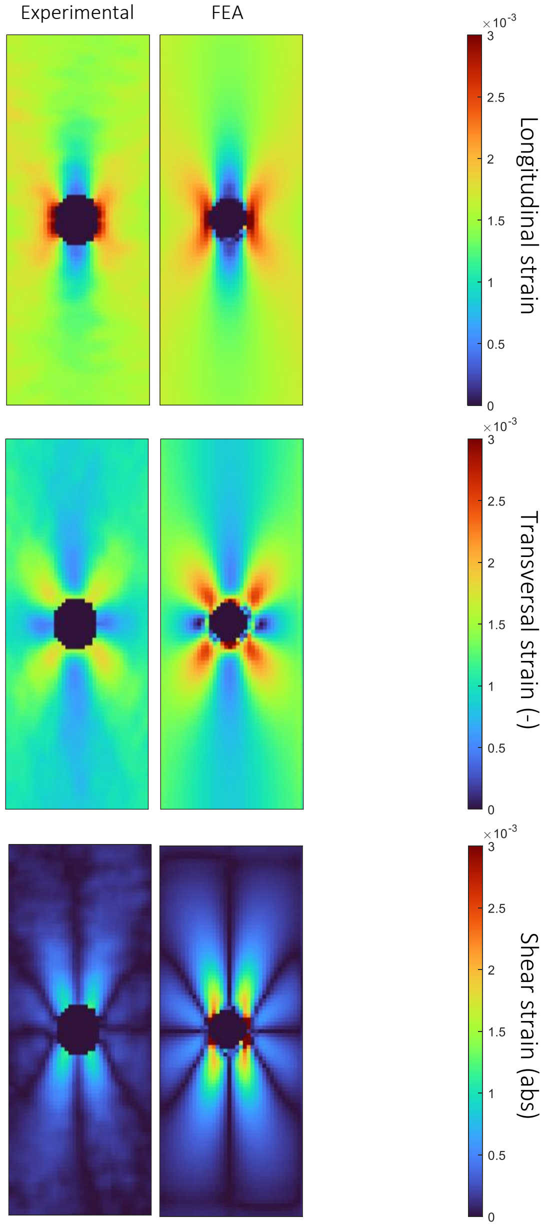

DIC Experimental strains – FEA Model strains

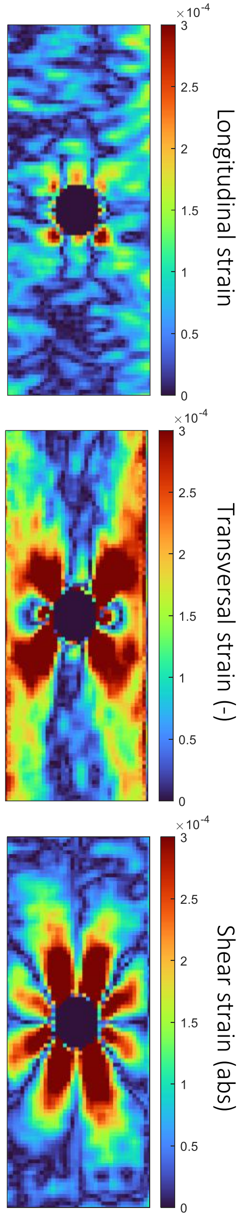

FEDEF

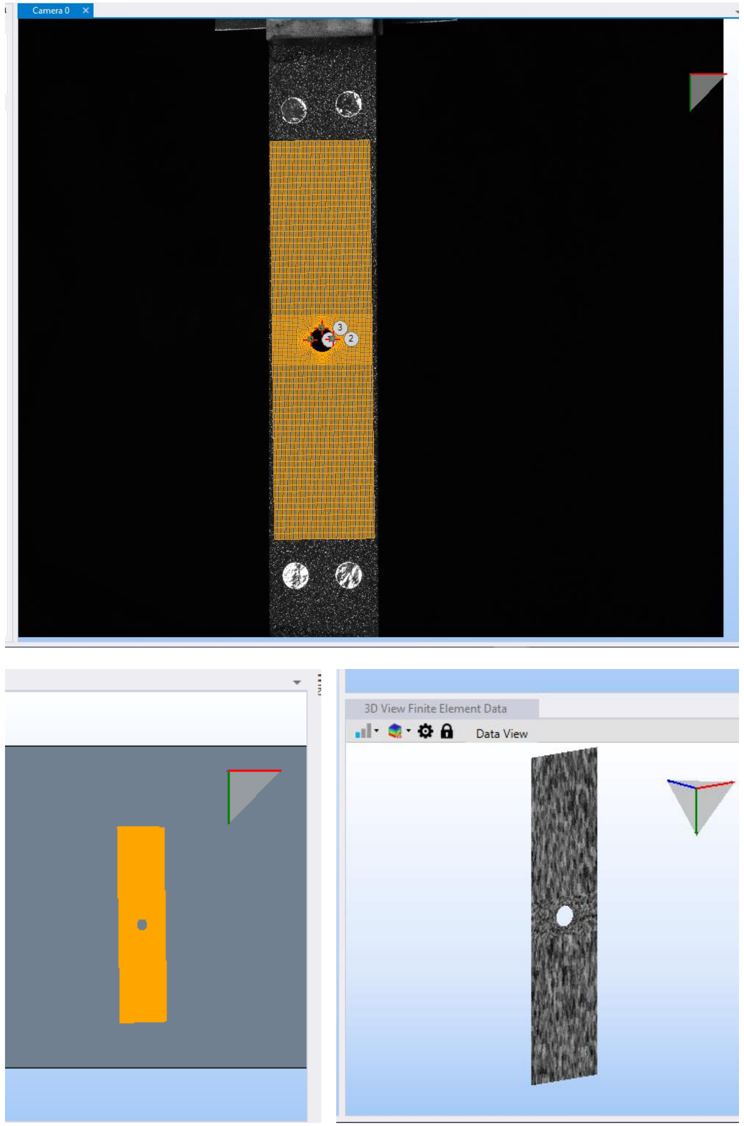

DIC Experimental strains – FEDEF strains